PHYSICAL REVIEW D **85,** 074011 (2012)

Strong decays of K_1 resonances

A. Tayduganov,[1,2] E. Kou,[1] and A. Le Yaouanc[2]

[1]*Laboratoire de l'Accélérateur Linéaire, Univ. Paris-Sud 11, CNRS/IN2P3 (UMR 8607), 91405 Orsay, France*

[2]*Laboratoire de Physique Théorique, CNRS/Univ. Paris-Sud 11 (UMR 8627), 91405 Orsay, France*

(Received 10 January 2012; published 10 April 2012)

We investigate the $K_1 \to K\pi\pi$ strong interaction decays. Using the $^3P_0$ quark-pair-creation model (QPCM) to derive the basic parametrization, we discuss in detail how to obtain the various partial wave amplitudes into the possible quasi-two-body decay channels as well as their relative phases from the currently available experimental data. We obtain the K_1 mixing angle to be $\theta_{K_1} \simeq 60°$, in agreement with previous works. Our study can be applied to extract the information needed for the photon polarization determination of the radiative $B \to K_1\gamma$ decay.

DOI: 10.1103/PhysRevD.85.074011 PACS numbers: 13.25.Es, 12.39.Jh, 14.40.Df

I. INTRODUCTION

A. Motivation for Revisiting K_1-Meson Strong Decays

A method has been proposed to measure the polarization of the photon in weak radiative decays of the B-meson by exploiting the decay $B \to K\pi\pi\gamma$, with the system $K\pi\pi$ resonating into a K_1 state [1,2]. We have recently extended this work [3] and have shown that exploiting the full Dalitz plot for the $K\pi\pi$ system could increase the sensitivity to the polarization determination inspired by the method of Davier *et al.*, introduced in Ref. [4]. For this purpose, it is important to have a good understanding of the strong K_1-decays. Indeed, it turned out that the $B \to K_1(1270)\gamma$ channel, not considered in the original works [1,2], dominates over $K_1(1400)$, [5] while the pattern of the partial wave is especially complex for $K_1(1270)$.

In the present paper, we give a detailed account and full discussion of the K_1 hadronic decays. The amplitude of the process $K_1 \to K\pi\pi$ can be described by the basic quantity $\vec{\mathcal{J}}$:

$$\mathcal{M}(K_1 \to K\pi\pi) \propto \vec{\varepsilon} \cdot \vec{\mathcal{J}}, \tag{1}$$

where $\vec{\varepsilon}$ is the polarization vector of the K_1 in the K_1 rest frame. The general framework for calculating $\vec{\mathcal{J}}$ is the *quasi-two-body approximation*: the process $K_1 \to K\pi\pi$ is decomposed into two steps: (1) the decay of $K_1 \to$ vector isobar (V) + pseudoscalar (P); (2) the decay of the vector isobar (K^* or ρ) into 2 pseudoscalars. Then, $\mathcal{J}$ is a sum of terms which are products of couplings and one isobar denominator.[1] The explicit expressions for $\mathcal{J}$ have been given in Ref. [3]. The decay properties of the intermediate isobars are well known. Here, we are then interested in evaluating the couplings describing the first step of the decay, $K_1 \to VP$, and the relative signs or phases between the various channels. Concerning our motivation, it has appeared that the determination of the polarization parameter, called λ_γ, of $B \to K_1\gamma$, depends essentially on the expression $\mathrm{Im}[\vec{n} \cdot (\vec{\mathcal{J}} \times \vec{\mathcal{J}}^*)]/|\vec{\mathcal{J}}|^2$ [1–3]. This expression vanishes unless complex phases are present in $\mathcal{J}$. These are mainly provided by the Breit-Wigner (BW) denominators of intermediate resonances (the so-called ''isobars''), and possibly by complex phases of the couplings. It is found that such a quantity is very sensitive to the relative signs of the various channels in the strong decay, whence it is important to determine the signs, or possibly, complex phases of the couplings, which anyway can be observed in the various experiments, provided one measures a sufficient number of angular distributions. One requires also specifically good knowledge of (1) D-waves; (2) off shell extrapolation.

B. Status of Experimental Study of K_1-Mesons

In principle, all the necessary hadronic parameters (i.e. K_1 masses and partial decay widths, form factors and relative phases) can be determined from fits to the experimental data. However, at present, we are far from being able to perform this with good accuracy; the experiments suffer from many drawbacks. The main reason is that the case under study cumulates many difficulties and complications, which have been underestimated in theoretical discussions:

(1) several possible partial waves (S, D) for the same channel
(2) three-body decay through multiple interfering channels
(3) broad parent K_1 resonances
(4) effect of the large widths of isobars K^* and ρ
(5) effect of a threshold ($K\rho$) close to the $K_1(1270)$ resonance
(6) overlapping and mixing of two close states, $K_1(1270)$ and $K_1(1400)$

Perhaps not surprisingly for this particularly complicated case, one observes a rather confusing situation in experiments (e.g. contrary statements on total widths, on

[1]In the full expression for the weak process, $\vec{\varepsilon} \cdot \vec{\mathcal{J}}$ has still to be multiplied by a production amplitude and the corresponding Breit-Wigner denominator for the K_1.

the $\kappa\pi$ decay channel, etc.). This has been causing misunderstandings on these important observables. Then, one cannot simply use, for example, the Particle Data Group (PDG) entries, as is done usually. One should return to the original papers to understand what is actually measured, and this is not always easy. And also, we noticed some definite weak points. Up to now, the most complete and accurate experimental analysis is the one by Daum *et al.* . It relies unhappily on the problematic phase-space treatment of Nauenberg and Pais for decays to isobars. One notes also the absence of nonresonant background in the K-matrix, and the presence of unexplained ''offset'' phases. All this is explained in detail in Sec. IV B. Finally, there is also lack of important information like the conventions of coupling signs or incomplete reports of the parameters of the fit. Other experiments, which have been mentioned previously, give precious complementary information, but they are not able to solve all the problems, especially because they are less accurate and include fewer physical features in their fits (e.g. neglect of D-waves). Therefore, a sizable part of our work has consisted of an extensive discussion of the experimental analyses (mainly the one of Daum *et al.* and the one of Belle [15]).

C. Theoretical Treatments of K_1-Mesons

The theoretical model has a first aim to give a physical understanding of the observed decay properties, which are far from trivial. In addition, it may serve to complement the experimental knowledge, where there are some lacks or weaknesses, and to help in future experimental analyses. Of course, there is no fundamental theoretical treatment of such processes. We have only phenomenological approaches at our disposal, mainly the one provided by the quark models. Approximate as it is, the quark model can be very precious to check the consistency of the present data and to orient the future studies of K_1-decays. However, we have to keep in mind that it suffers from inherent, sizable, and unknown uncertainties, which could limit the accuracy of the λ_γ determination as mentioned previously. To our knowledge, the best phenomenological model in the present case of K_1-decays is the family of quark models that are able to master the large set of hadronic states and their decays with a limited number of adjusted parameters.[2]

Admittedly, quark models are many, but one must distinguish among the potential models and the decay models. The diversity is especially one of potential models, which intend to describe the spectroscopy of states. As concerns decays, there are not so many basic models. In fact, there are elementary emission models and quark-pair-creation models, both concerning two-body decays. This is why the quasi-two-body decay assumption is a natural step in the theoretical treatment of the three-body decay. The quark-pair-creation models have the advantage of unifying the whole of two-body and quasi-two-body decays. Among them, the $^3P_0$ model (see Sec. III B and references therein) is particularly favored as being the easiest to handle and the more extensively tested, with a striking overall success over hundreds of decays. We use the $^3P_0$ model with the important additional input of a damping factor to account for off shellness. Of course, as said previously, quark models are inherently approximate. As to the proper decay model, the main problem is that it is essentially nonrelativistic, which is of course in principle very far from the real situation. It has been known for quite a long time that, quite surprisingly, nonrelativistic decay or emission models may work well, but their accuracy cannot be estimated *a priori*; it has always to be judged *a posteriori*. Decay models must be necessarily combined with potential models, giving the wave functions that must be folded into their general structure. In view of the rather naive status of the $^3P_0$ model, we do not find it appropriate to use a sophisticated set of wave functions, but rather a simple one, as explained in Sec. III B. We must underline, however, that the oscillator radii that are used are not at all free parameters: They have to be fixed on the actual spectrum. On the other hand, the model contains free phenomenological parameters; namely, the mixing angle of K_1 states, θ_{K_1}, and the quark-pair-creation constant γ. These parameters are to be adjusted on the strong decay experiments themselves (additional information on the mixing can be obtained from the mass spectrum or other types of decays).

D. Plan of the Paper

In Sec. II, we present a brief summary of the present status of the experience concerning the K_1-mesons. In Sec. III, after having discussed the basic question of the mixing, we introduce the formalism of the theoretical model; namely, the $^3P_0$ quark-pair-creation model, used to predict the partial wave amplitudes for the quasi-two-body decays of the K_1-meson. In Sec. IV, we establish the general relation between our model predictions and the most extensive experimental results obtained by the ACCMOR Collaboration [8], which uses the K-matrix formalism to analyze the partial waves. We describe some of the problems we have observed, which include the definition of the total K_1-width, the phase space and threshold effects, the strong phase between different intermediate resonance (isobar) states. In Sec. V, combining the experimental results on the K_1-decays and the predictions of the quark-pair-creation model, we determine the phenomenological parameters of this decay model, the K_1 mixing angle θ_{K_1} and the universal quark-pair-creation constant γ, and we present the resulting numerical predictions. We compare our model predictions and the measurements of the ACCMOR [8] and Belle Collaborations. [15] We also discuss the issues of the relative strong offset

[2]See Ref. [6] for another approach based on phenomenological Lagrangian.

TABLE I. Fitted masses, total widths, and partial branching ratios of $K_1(1^+)$ decays into vector-pseudoscalar states, measured by the ACCMOR Collaboration in the $Kp \to K\pi\pi p$ reaction for the low momentum transfer to the recoiling proton [8], and tabulated in PDG. The total widths seem to be misleading for the calculation of partial widths, as discussed later in the text.

K_1	$M_{K_1}^{\mathrm{ACCMOR}}$, GeV/$c^2$	$\Gamma_{K_1}^{\mathrm{ACCMOR}}$, MeV/$c^2$	$\mathcal{B}(K^*\pi)_S$	$\mathcal{B}(K^*\pi)_D$	$\mathcal{B}(K\rho)_S$
$K_1(1270)$	1.27 ± 0.007	90 ± 8	0.13 ± 0.03	0.07 ± 0.006	0.39 ± 0.04
$K_1(1400)$	1.41 ± 0.025	165 ± 35	0.87 ± 0.05	0.03 ± 0.005	0.05 ± 0.04

phases and the controversial $K_1(1270) \to \kappa\pi$ channel. We give our conclusions and perspectives in Sec. VI.

II. OVERVIEW OF PREVIOUS EXPERIMENTAL K_1-DECAY STUDIES

Here we summarize the experimental results of the axial vector K_1-resonance study.

(1) Two close in mass axial-vector mesons, $K_1(1270)$ and $K_1(1400)$, were disentangled in the experiments on the diffractive production of the $1^+(K\pi\pi)$ system in the $Kp \to K\pi\pi p$ reaction, first by the group at SLAC [7] and then by the ACCMOR Collaboration in the WA3 experiment at CERN [8]. They also observed separately, one $K_1(1270)$ in the strangeness-exchange reaction $\pi^- p \to \Lambda K\pi\pi$ [9] and the other $K_1(1400)$ in the charge-exchange reaction $K^- p \to \bar{K}^0\pi^+\pi^- n$ [10]. In our study we rely mainly on the diffractive reactions which allow a more detailed study. The relative ratios of two dominant channels, $K^*\pi$ and $K\rho$, indicate that $K_1(1400)$ decouples from the $K\rho$, while the $K\rho$ decay mode of $K_1(1270)$ is dominant (see Table I). This decay pattern suggests that the observed mass eigenstates, $K_1(1270)$ and $K_1(1400)$, are the mixtures of two strange axial-vector $SU(3)$ octet states, $K_{1A}(^3P_1)$ and $K_{1B}(^1P_1)$, as we will explain.

(2) The K_1-resonances were also observed and studied in τ-decays, $\tau \to K_1\nu_\tau$, by the TPC/Two-gamma [11], ALEPH [12], OPAL [13], and CLEO [14] Collaborations.

(3) Radiative B-decays involving the K_1-mesons were also observed by the Belle Collaboration [5]. The data indicate that $\mathcal{B}(B \to K_1(1270)\gamma) \gg \mathcal{B}(B \to K_1(1400)\gamma)$.

(4) Quite recently the Belle Collaboration published a paper on $B \to J/\psi(\psi')K\pi\pi$ decays [15], which will be discussed in detail at another point in this paper.

(5) In addition, the *BABAR* Collaboration reported the measurement of the branching ratios of neutral and charged B-meson decays to final states containing a $K_1(1270)$ and $K_1(1400)$-meson and a charged pion: $B^0 \to K_1(1270/1400)^+\pi^-$ and $B^+ \to K_1(1270/1400)^0\pi^+$ [16]. In order to parametrize the signal component for the production of the K_1-resonances in B-decays, the K-matrix formalism, used in the analysis by Daum *et al.* in Ref. [8], was applied for the model description. Since only some parameters used in the analysis of the ACCMOR Collaboration have been reported, the *BABAR* Collaboration refitted the ACCMOR data in order to determine the parameters describing the diffractive production of the K_1-mesons and their decays. One observes that some results are somewhat different.

III. THEORETICAL MODEL

Before presenting the $^3P_0$, we begin by explaining the question of the mixing of K_1 states, which is a basic assumption of all the approaches, since there is no theoretical approach predicting this mixing quantitatively.

A. Mixing of K_1 Resonances

In the quark model, there are two possible states for the orbitally excited axial-vector mesons: $J^{PC} = 1^{++}$ and $J^{PC} = 1^{+-}$, depending on different spin couplings of two constituent quarks. In the $SU(3)$-limit, these states do not mix in general, but since the s-quark is actually heavier than the u- and d-quarks, the observed $K_1(1270)$- and $K_1(1400)$-mesons are not pure 1^3P_1 or 1^1P_1 states. They are considered to be mixtures of nonmass eigenstates K_{1A} and K_{1B}. Introducing a $K_{1A} - K_{1B}$ mixing angle θ_{K_1}, mass eigenstates can be defined in the following way [17][3]:

[3]To be able to compare with other mixing angle estimations, one has to be careful due to the different parametrizations that are used in the literature. For instance, in the analysis by Carnegie *et al.* [7], the parametrization is $|K_1(1270)\rangle = |K_{1A}\rangle\cos\theta_{K_1}^{(\mathrm{SLAC})} + |K_{1B}\rangle \times \sin\theta_{K_1}^{(\mathrm{SLAC})}$, $|K_1(1400)\rangle = -|K_{1A}\rangle\sin\theta_{K_1}^{(\mathrm{SLAC})} + |K_{1B}\rangle\cos\theta_{K_1}^{(\mathrm{SLAC})}$. To compare with the results made by Daum *et al.* [8], parametrization is written as follows: $|K_1(1270)\rangle = -|K_{1A}\rangle\sin\theta_{K_1}^{(\mathrm{ACCMOR})} + |K_{1B}\rangle\cos\theta_{K_1}^{(\mathrm{ACCMOR})}$, $|K_1(1400)\rangle = |K_{1A}\rangle\cos\theta_{K_1}^{(\mathrm{ACCMOR})} + |K_{1B}\rangle\sin\theta_{K_1}^{(\mathrm{ACCMOR})}$. Comparing the fitted effective couplings, one can see that the coupling to K_{1B} has a different sign in these two definitions. Since one can measure only the absolute value of the amplitude, this sign changes nothing, and hence it is possible to redefine the sign of this coupling in the paper by Daum *et al.* . After that, one can easily establish the correspondence between these two forms of parametrization and the one we use in this paper: $\theta_{K_1} = \theta_{K_1}^{(\mathrm{ACCMOR})} = 90^\circ - \theta_{K_1}^{(\mathrm{SLAC})}$.

$$|K_1(1270)\rangle = |K_{1A}\rangle \sin\theta_{K_1} + |K_{1B}\rangle \cos\theta_{K_1}$$
$$|K_1(1400)\rangle = |K_{1A}\rangle \cos\theta_{K_1} - |K_{1B}\rangle \sin\theta_{K_1} \quad (2)$$

Since all of $SU(3)$ operators can be expressed as combinations of isospin, U- and V-spin operators, if an operator describing the interaction is invariant under the $SU(3)$-group transformations, it is also invariant under the isospin, U-spin and V-spin transformations [18]. However, it is sufficient to require the invariance only under the isospin and U-spin (or V-spin) transformations, since V-spin is dependent on the isospin and U-spin, and the V-spin operators can be obtained from the U-spin operators by an isospin transformation (U-spin can be turned into V-spin via rotation by 120°).

Analogously to G-parity, one can define U- and V-parities: $G_U = C(-1)^U$ and $G_V = C(-1)^V$, respectively, where C is the charge-conjugation parity of the neutral nonstrange members of the multiplet. The neutral and charged kaons in the octets are the eigenstates of U- and V-parities and always have U or $V = 1$, respectively.

In the $SU(3)$-limit, two kaons that belong to the octets of the same spin but opposite C-parity cannot mix. To illustrate, one can consider a matrix element of some arbitrary operator $\mathcal{O}$ between two neutral kaons from different octets [19,20]:

$$\langle K_A|\mathcal{O}|K_B\rangle = \langle K_A|G_U^{-1}G_U\mathcal{O}G_U^{-1}G_U|K_B\rangle = C_A C_B\langle K_A|G_U\mathcal{O}G_U^{-1}|K_B\rangle \quad (3)$$

If the $\mathcal{O}$ operator is $SU(3)$-invariant, i.e. $G_U\mathcal{O}G_U^{-1} = \mathcal{O}$, the matrix element of the transition $\langle K_A|\mathcal{O}|K_B\rangle = 0$ unless $C_A = C_B$.

Strong interactions can break the $SU(3)$-symmetry and produce the mass splittings. It is experimentally confirmed that isospin is conserved in strong interactions. Hence, if the strong interaction operator breaks the $SU(3)$-symmetry, U- and V-parities are not conserved anymore, even if G-parity is conserved. In this case $G_U\mathcal{O}G_U^{-1} \neq \mathcal{O}$ and consequently $\langle K_A|\mathcal{O}|K_B\rangle \neq 0$ and the mixing takes place.

That this mixing is indeed the effect of the symmetry breaking can be explicitly seen in quark models at the level of bound states of a potential model. It is induced, for instance, by spin-orbit forces with different s and u, d quark masses. A mixing is also generated by the two-meson loops due to quark pair creation and annihilation in the bound states, as is explained in the K-matrix approach, Sec. IV A. In this approach, the real mixing must be understood as one of the K-matrix couplings corresponding to the effect of the real part of the loops, while additional complex mixing would be present in the physical couplings.

One can see easily why the loops and the $SU(3)$ breaking generate mixing. For instance, the $K^*\pi$ and $K\rho$ loop contributions connect the K_A and the K_B, since both states are coupled to these channels. In this way, it generates mixing. The two contributions cancel each other if one sets $M_{K^*} = M_\rho$ and $m_\pi = m_K$, i.e. in the case of the exact $SU(3)$-symmetry. It must be emphasized, however, that this mechanism of loops does not lead to the actual calculation of the mixing angle, because one would have to sum over a very large number of possible intermediate states. Therefore, in this approach, it remains an independent phenomenological parameter, which has to be fixed through confrontation with data.

It is to be noted that, in any case, no fundamental calculation of the mixing has been produced.

Previous Phenomenological Determinations of Mixing Angle

Here, we gather all the various estimations of θ_{K_1}.

On the other hand, there have been in the past many attempts to determine the mixing angle, both from experimentalists and theoreticians, but in both cases only through phenomenological analyses. The phenomenological analyses have concerned the masses (with additional assumptions, since $SU(3)$ alone does not enable us to fix the mixing angle from the masses), the $\tau \to K_1\nu_\tau$ decays, the $B \to K_1$ transitions, and mainly the strong decays $K_1 \to K\pi\pi$ through $K^*\pi$ and $K\rho$ channels. Indeed, the pattern of the latter is very sensitive to the mixing angle.

The angles are given according to the definition in Eq. (2). However, one must warn that it does not completely fix the definition, since there may be different choices of the phases of the states. In general, it is difficult to establish completely the connection to our own definition in the present paper, so we only state the absolute magnitude of the angle.

(1) In the experiment, carried out at SLAC by Carnegie *et al.* [7], the mixing angle was determined from the $SU(3)$ couplings to the $K^*\pi$ and $K\rho$ channels to be $\theta_{K_1} = (41 \pm 4)°$. On the other hand, the partial wave analysis of the WA3 experiment data, done by the ACCMOR Collaboration (Daum *et al.* [8]), gives $\theta_{K_1} = (64 \pm 8)°$ and $\theta_{K_1} = (54 \pm 4)°$ for the low and high momentum transfer, respectively, to the recoiling proton.

(2) In the reanalysis of ACCMOR data by *BABAR* [16], using the low t-data, the refitted value of the K_1 mixing angle turns out to be 72° compared to 64° from the ACCMOR fit.

(3) In the work by Suzuki [17], the mixing angle is determined by three different approaches. One is to explain the observed hierarchy in the K_1 strong decays to $K^*\pi$ and $K\rho$, as has been done by SLAC [7] and ACCMOR. [8] Another is the $SU(3)$ analysis of the masses of the two octets, but with additional assumptions. Finally, the suppression of

$\tau \to K_1(1400)\nu$ with respect to $\tau \to K_1(1270)\nu$ is considered. Two possible solutions for the K_1 mixing angle were found: $\theta_{K_1} \approx 33°$ or $57°$.

(4) In the analysis of $\tau \to K_1\nu$ done by the CLEO Collaboration [14], the K_1 mixing angle was determined from the measured ratio $\mathcal{B}(\tau \to K_1(1270)\nu_\tau)/\mathcal{B}(\tau \to K_1(1400)\nu_\tau)$: $\theta_{K_1} = (69 \pm 16 \pm 19)°$ for $\delta = 0.18$ and $\theta_{K_1} = (49 \pm 16 \pm 19)°$ for $\delta = -0.18$, where $|\delta| = \frac{m_s - m_u}{\sqrt{2}(m_s + m_u)} \approx 0.18$ is a phenomenological $SU(3)$ breaking parameter. This result is consistent with the calculation by Suzuki [17].

(5) In the work of Blundell, Godfrey, and Phelps [21],

(a) The mixing is discussed using the results of the TPC/Two-gamma Collaboration: $\mathcal{B}(\tau^- \to K_1(1270)^-\nu_\tau) = (0.41^{+0.41}_{-0.35})\%$ and $\mathcal{B}(\tau^- \to K_1(1400)^-\nu_\tau) = (0.76^{+0.40}_{-0.33})\%$. This would seem to mean that the rate into $K_1(1400)$ is larger than that into $K_1(1270)$, although their errors are too large to make a strong statement. At any rate, these numbers have been superseded by the CLEO data, which show the contrary.

(b) The strong decays of the K_1-mesons to the final states $K^*\pi$ and $K\rho$ were studied as well in order to determine the mixing angle. A χ^2 fit of the experimental data on the partial decay widths $\Gamma(K_1(1270/1400) \to K^*\pi)$ and $\Gamma(K_1(1270/1400) \to K\rho)$ was used for the θ_{K_1}-determination.

(i) Performing a χ^2-fit with the predicted decay widths, calculated within the pseudoscalar-meson-emission model using simple harmonic oscillator wave functions with a single parameter $\beta = 0.40$ GeV, the fitted value of the mixing angle was obtained: $\theta_{K_1} = (48 \pm 5)°$.

(ii) The strong K_1-decays were also calculated using both the flux-tube-breaking model and the $3P_0$ model for several sets of meson wave functions. In all cases, a second fit was performed by allowing both θ_{K_1} and the quark-pair-creation constant γ to vary, which reduces the χ^2 significantly. Using simple harmonic oscillator wave functions with $\beta = 0.40$ GeV, comparison of the predicted decay widths by the $^3P_0$ model to experimental results gives $\theta_{K_1} = (45 \pm 4)°$, while the flux-tube-breaking model's prediction gives $\theta_{K_1} = (44 \pm 4)°$, both appreciably different from our central value $\theta_{K_1} \simeq 60°$ with the same set of wave functions. Their last result for θ_{K_1} is slightly changed in the case of use of a different set of the meson wave functions from Ref. [22]: $\theta_{K_1} = (51 \pm 3)°$.

(6) A detailed study of the $B \to K_1(1270)\gamma$ and $B \to K_1(1400)\gamma$ decays in the light-cone QCD sum rules approach was presented by Hatanaka and Yang in Ref. [23]. The sign ambiguity of the mixing angle is resolved by defining the signs of the decay constants $f_{K_{1A}}$ and $f^\perp_{K_{1B}}$.

(a) From the comparison of the theoretical calculation and the data for decays $B \to K_1\gamma$ and $\tau \to K_1\nu_\tau$, it was found that $\theta_{K_1} = -(34 \pm 13)°$ is favored within the conventions of Hatanaka and Yang. It is difficult to establish the relation with our own convention as regards sign.

(b) The predicted branching ratios, $\mathcal{B}(B \to K_1(1400)\gamma)$ and $\mathcal{B}(B \to K_1(1270)\gamma)$, are then in agreement with the Belle Collaboration [5] measurement, within the errors.

In summary, the cleanest way to extract the mixing angle is certainly, in principle, the determination from the ratio of $\mathcal{B}(\tau \to K_1(1400/1270)\nu_\tau)$, if the data were sufficiently accurate. At present, we believe that the best way remains the study of strong decays, as we do in this paper.

B. $^3P_0$ Quark-Pair-Creation Model

There are several additive quark models of strong vertices. All these models relate to the recoupling coefficients of unitary spin, quark spin, and the quark orbital angular momenta, but differ in the dynamical description. One of the simplest additive quark models describing three-meson vertices is the naive quark-pair-creation model (QPCM), with a $^3P_0$ structure for the pair, formulated by Le Yaouanc, Oliver, Pène, and Raynal [24], starting from ideas of Micu and of Carlitz and Kislinger [25,26]. The model has then been extensively applied and discussed by many authors, including the same authors (see Ref. [27] and some references therein) and the group of N. Isgur in Canada (for instance, Refs. [28,29]). As in the usual additive quark models with spectator quarks, the quark-antiquark pair is naively created not from the ingoing quark lines but within the hadronic vacuum. The strong interactions vertices in the QPCM are expressed in terms of the explicit harmonic oscillator spacial $SU(6)$ wave functions (compared to the work by Micu [25], who just fitted the various spacial integrals using the measured decay widths, which does not allow to study the polarization effects) and a nonlocal vacuum quark-antiquark pair production matrix element, depending on the internal quark momenta (while Carlitz and Kislinger [26] neglected the internal momentum distributions). Contrary to the QPCM by Colglazier and Rosner [30], the $^3P_0$ structure of the created pair describes any decay process of any hadron, using one universal parameter. The other model parameters are those of the hadrons themselves (potential model), and not relative to the decay process as in Ref. [30], where the various extra couplings between the pair and the incoming meson depend on the nature of the hadron states and may be weighted by different arbitrary coefficients for different hadrons.

The naive QPCM has the advantage of making definite predictions for all hadronic vertices; moreover, contrary to the other works, it predicts the relative signs of the couplings. Another appealing feature of the model is that it consists of only one phenomenological parameter (the quark-pair-creation constant), which allows a much more general description and relates the amplitudes of different processes. The main weakness of the QPCM is that the emitted hadrons are considered to be nonrelativistic. Thus, one has to look for the decays that are not significantly sensitive to these effects.

A specific study of the strange axial-vector mesons was first done by Blundell, Godfrey, and Phelps [21], who studied the properties of K_1 by combining wave functions inspired by the Godfrey-Isgur quark model [22]to describe the bound states, and the flux-tube-breaking or $^3P_0$ models to describe the decays. Although we start from the same basic $^3P_0$ model, we give a much more extended study, which is in particular required for the purpose of the λ_γ determination. We make a rather different discussion, especially, for the relation between theory and experiment. We clarify the relation with the K-matrix analysis, which is the tool used by the main experiment; that is, the ACCMOR experiment. [8] We discuss the definition of widths, which appears very ambiguous due to threshold effects. We also include a treatment of the off shellness (i.e., damping factor). In addition, we explore the system of phases, which is one main achievement of the model (as well as the fact that it has been in the baryon decays). Finally, we discuss in detail the most problematic $\kappa\pi$ channel. These differences will become apparent from the rest of the paper.

1. Formalism

In the QPCM, instead of being produced from the gluon emission, the quark-antiquark pair $q\bar{q}$ (see Fig. 1) is created anywhere within the hadronic vacuum by an operator proportional to $(u\bar{u} + d\bar{d} + s\bar{s})\mathbf{S}\cdot\mathbf{p}$, where $\mathbf{S}$ refers to spin 1 and $\mathbf{p}$ is the relative momentum of the pair. It is combined with the initial quark-antiquark system $\bar{q}_2 q_1$ and produces the final state $B(q_1\bar{q})C(q\bar{q}_2)$. The initial spectator quarks

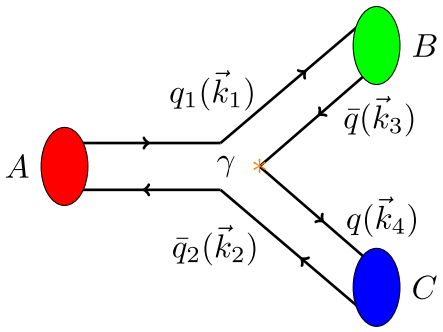

FIG. 1 (color online). Three-meson vertex in the quark-pair-creation model.

are not supposed to change their $SU(3)$ quantum numbers, nor their momentum and spin. In order to conserve the vacuum quantum numbers, the pair must be created in the $^3P_0$ state due to $P = -(-1)^L$ and $C = (-1)^{L+S}$ parity conservation with 0-total momentum ($\vec{k}_3 + \vec{k}_4 = 0$) and must be a $SU(3)$-singlet. Thus the matrix element of the quark-antiquark pair production from the vacuum is unambiguously constructed with the help of the spins and momenta of the quark and antiquark only [24]:

$$\langle \bar{q}q|\hat{T}_{\rm vac}|0\rangle = \delta(\vec{k}_3 + \vec{k}_4)\gamma\sum_m (1, m; 1, -m|0, 0) \times \mathcal{Y}_1^m(\vec{k}_3 - \vec{k}_4)\chi_1^{-m}\phi_0 \tag{4}$$

where γ is a phenomenological dimensionless pair-creation constant (which is determined from the measured partial decay widths and taken to be of the order of 3–5), χ_1^{-m} are the spin-triplet wave functions, $\phi_0 = \frac{1}{\sqrt{3}}(u\bar{u} + d\bar{d} + s\bar{s})$ is the $SU(3)$-singlet, and $\mathcal{Y}_1^m$ represents the $L = 1$ angular momentum of the pair.

Taking the matrix element of the pair-creation operator between the $SU(6)$ harmonic-oscillator wave functions of hadrons, the matrix element for the decay $A \to B + C$ can be written as:

$$\langle BC|\hat{T}|A\rangle = \gamma\sum_m (1, m; 1, -m|0, 0)\Phi_B\Phi_C\Phi_A^m\Phi_{\rm vac}^{-m} I_m^{(ABC)}, \tag{5}$$

where $\Phi = \chi_1^m\phi$ are the $SU(6)$ spin-flavor wave functions and $I_m^{(ABC)}$ are the spatial integrals dependent on the momentum of the final states, which are computed in Appendix B.

Assuming A, B, and C to be an axial vector, pseudoscalar, and vector mesons respectively, the spin part of the matrix element can be written as

$$\begin{aligned}\chi_C\chi_B\chi_A\chi_{\rm pair} &= \sum_{m_i}\left(\frac{1}{2}, m_1; \frac{1}{2}, m_3|0, 0\right)\left(\frac{1}{2}, m_4; \frac{1}{2}, m_2|1, \lambda_C\right) \\ &\times \left(\frac{1}{2}, m_1; \frac{1}{2}, m_2|S_A, m_{S_A}\right)(1, m_{L_A}; S_A, m_{S_A}|1, \lambda_A) \\ &\times \left(\frac{1}{2}, m_4; \frac{1}{2}, m_3|1, -m\right)\end{aligned} \tag{6}$$

Consider, for instance, $K^{*0}\pi^+$ decay mode of K_1-meson. After the summation over the spin projections, the calculated helicity amplitudes for the K_{1A} (1^3P_1) and K_{1B} (1^1P_1) will be (the definition of the helicity amplitudes and their relation with the partial wave amplitudes can be found in Appendix C):

TABLE II. Partial wave amplitudes of $K_{1A}(1^3P_1)$ and $K_{1B}(1^1P_1)$ decays into vector-pseudoscalar states, calculated within QPCM.

Decay mode	A_S	A_D
$K_{1B} \to K^*\pi$	$-S^{(K_1K^*\pi)}$	$-\sqrt{2}D^{(K_1K^*\pi)}$
$K_{1A} \to K^*\pi$	$\sqrt{2}S^{(K_1K^*\pi)}$	$-D^{(K_1K^*\pi)}$
$K_{1B} \to K\rho$	$S^{(K_1K\rho)}$	$\sqrt{2}D^{(K_1K\rho)}$
$K_{1A} \to K\rho$	$\sqrt{2}S^{(K_1K\rho)}$	$-D^{(K_1K\rho)}$

$$\mathcal{M}_{00}^{10(A)} = -\gamma\frac{I_1^{(K_1K^*\pi)}}{3\sqrt{2}}, \quad \mathcal{M}_{10}^{11(A)} = -\gamma\frac{I_1^{(K_1K^*\pi)} - I_0^{(K_1K^*\pi)}}{6\sqrt{2}}$$
$$\mathcal{M}_{00}^{10(B)} = -\gamma\frac{I_0^{(K_1K^*\pi)}}{6}, \quad \mathcal{M}_{10}^{11(B)} = \gamma\frac{I_1^{(K_1K^*\pi)}}{6} \tag{7}$$

The corresponding amplitudes for the $K^+\rho^0$ mode are obtained by multiplying the $K^{*0}\pi^+$ amplitudes by $1/\sqrt{2}$ and changing the sign of K_{1A}-part.

Taking into account the isospin factors for different charge states,[4] the generalized amplitudes are summarized in Table II. The functions S and D are defined as

$$S^{(ABC)} = \gamma\sqrt{\frac{3}{2}}\frac{2I_1^{(ABC)} - I_0^{(ABC)}}{18},$$
$$D^{(ABC)} = \gamma\sqrt{\frac{3}{2}}\frac{I_1^{(ABC)} + I_0^{(ABC)}}{18}. \tag{8}$$

One has to point out that our treatment obeys the $SU(3)$-symmetry. $SU(3)$ breaking effects are present only in two places: (1) We use the physical observed masses of hadrons to calculate the momentum transfer of the decay and the phase space; (2) We introduce mixing between the K_{1A} and K_{1B} states.

Then the decay amplitudes of the physical K_1 states into $K^*\pi$ or $K\rho$ final states can be expressed as functions of the pseudoscalar meson momentum in the K_1 reference frame and the mixing angle θ_{K_1}:

$$\begin{aligned}
A_S(K_1(1270) \to K^*\pi/K\rho) &= S^{(K_1K^*\pi/K_1K\rho)}(\sqrt{2}\sin\theta_{K_1} \mp \cos\theta_{K_1}) \\
A_D(K_1(1270) \to K^*\pi/K\rho) &= D^{(K_1K^*\pi/K_1K\rho)}(-\sin\theta_{K_1} \mp \sqrt{2}\cos\theta_{K_1}) \\
A_S(K_1(1400) \to K^*\pi/K\rho) &= S^{(K_1K^*\pi/K_1K\rho)}(\sqrt{2}\cos\theta_{K_1} \pm \sin\theta_{K_1}) \\
A_D(K_1(1400) \to K^*\pi/K\rho) &= D^{(K_1K^*\pi/K_1K\rho)}(-\cos\theta_{K_1} \pm \sqrt{2}\sin\theta_{K_1}).
\end{aligned} \tag{9}$$

Correspondingly, the partial decay widths can be determined by using amplitudes squared from Eq. (9) multiplied by the phase-space factors:

$$\Gamma_{S/D}^{\mathrm{QPCM}}(K_1 \to VP) = 8\pi^2\frac{E_VE_Pk_P}{M_{K_1}}|A_{S/D}(K_1 \to VP)|^2. \tag{10}$$

Note that all the signs in the expressions for amplitudes make sense only within definite specific conventions. The ones in our work are defined in Appendix B. On the other hand, the signs of the products of the couplings of the two successive decay processes from the same K_1 state—that is, when we multiply by the decay amplitude of the isobar—make sense and the relative signs are observable because the final state $K\pi\pi$ is the same, and all phase arbitrariness cancels. It is an important feature of the model that *it can predict all these observable signs*. As will be seen in Sec. V C, these predictions are remarkably verified by experimental data.

2. Choice of Spatial Wave Functions

The unknown parameters of the model are the quark-pair-creation constant γ and the K_1 mixing angle, which we determine by fitting the experimental data on the K_1-decays (see the next section). However, before proceeding to this determination, the model must be specified by the choice of the set of meson wave functions. In accordance with the fact that the $^3P_0$ model is a simple model, we will remain within the traditional $SU(6)$ approximation, which describes rather well ordinary radiative decays (e.g. $\omega \to \pi\gamma$). This includes the $SU(3)$-symmetry approximation, which in any event is also present in the $^3P_0$ model through the fact that the quark-pair-creation constant is the same for all reactions. In this approach, the effect of the $SU(3)$ breaking is taken into account only through the dependence of the decay momentum of the physical hadronic masses. For practical reasons, we choose a set of harmonic oscillator wave functions, which are known to give a reasonable approximation.

Here one has to stress that the harmonic oscillator radius of the meson wave function [$\psi(r) \propto \exp(-r^2/2R^2)$; for details see Appendix B] is not a free phenomenological parameter. In principle, it can be predicted by the quark-potential model describing the bound states of two quarks.

[4]The amplitudes were calculated for $K_1^+ \to K^{*0}\pi^+$ and $K_1^+ \to K^+\rho^0$. The amplitude of $K\rho$ must be divided over $\sqrt{2}$ due to isospin wave function of ρ^0. To obtain the general amplitude, which does not depend on the charge combination, one has to divide over the isospin factor: $-\sqrt{2/3}$ for K^* and $\sqrt{1/3}$ for ρ, since for matching with the relativistic form factors the charge combination is not relevant. Finally one obtains the factor $\sqrt{3/2}$ in Eq. (8).

To get a first and rough estimate, we can use the following relation, obtained in the nonrelativistic harmonic oscillator model for the energy shift between the ground state and the first radial excitation:

$$\Delta E_1 = \frac{2}{m_q R^2}, \tag{11}$$

with m_q being the quark mass, which can be standardly estimated from the magnetic moment of the proton, $\mu_p = \frac{e}{2m_q} = \frac{2.79}{2m_N}$, whence $m_q \simeq 0.34$ GeV. ΔE_1 can be estimated from the energy of the $L = 1$ state of the order of (1.2–1.3) GeV and the weighted average energy of the ground state $(3m_\rho + m_\pi)/4 \simeq 0.6$ GeV. Then the estimated radius is given by

$$R = \sqrt{\frac{2}{\Delta E_1 m_q}} \sim \sqrt{\frac{2}{(1.25 - 0.6)0.34}} \simeq 3\ \text{GeV}^{-1} \tag{12}$$

On the other hand, it is obvious that this approximation of the Schroedinger equation with the harmonic oscillator potential is rather naive: The realistic potential is known to be of the form of linear (that describes confinement) plus Coulomb potential. One also has to notice that the application of the use of the nonrelativistic character of the Schroedinger equation to the heavy-light systems is dubious. Therefore, one could take a value inspired by the well-known model of Godfrey and Isgur [22]. Of course, in the latter model the solutions are no longer the harmonic oscillator wave functions. However, such harmonic oscillator wave functions can represent a good approximation if the radius R is adjusted. For most $L = 0, 1$ states, one finds in this model the typical value $R \sim 2.5\ \text{GeV}^{-1}$ [28]. For our predictions we therefore adopt a set of wave functions with a common harmonic oscillator radius having precisely this value,

$$R = 2.5\ \text{GeV}^{-1}. \tag{13}$$

This is one of the choices made by Blundell *et al.* [21]. We must warn that in the model of Godfrey and Isgur [22], pion and kaon have actually quite smaller radii ($\sim 1.4\ \text{GeV}^{-1}$ [28]) due to the strong spin-spin interaction force. If we were adopting the low values for the Goldstone boson, we would obtain unsatisfactory results. For example, using $R_\pi \simeq 1.4\ \text{GeV}^{-1}$, we cannot reproduce correctly the D/S ratio in the $b_1 \to \omega\pi$ decay, which is precisely measured ($D/S = 0.28$). The use of the exact wave functions of the model of Godfrey and Isgur [22] does not seem to improve the situation; one finds $D/S = 2.5/14 \simeq 0.18$ from the tables of Kokoski and Isgur [28].

Of course, although it has not been commented upon in previous works, this fact is disturbing, since the spin-spin force is present indeed in spectroscopy, and therefore it should be more realistic to include its effect. In addition to empirical success, the choice of equal radii can be motivated in the spirit of the $SU(6)$ approach. It must be remembered indeed that using the old quark model, very naive calculations have succeeded well with this $SU(6)$ symmetry, for instance, to relate $\omega \to \pi\gamma$ to magnetic moments. Now, the $^3P_0$ model is also in this very naive spirit: It is nonrelativistic in essence.

C. Issue of Damping Factor

In the end of this introduction, of the theoretical model, we discuss the necessity of introducing an additional cutoff on momenta (or damping factor) in the coupling vertices. Generally speaking, there is need for a strong cutoff for calculations involving far off shell particles once the model has been adjusted on real decays. Indeed, the natural falloff provided by simple continuation of the $^3P_0$ model, due to the wave functions, is seen to be much too weak. The need for this cutoff appears in various circumstances:

(i) In the branching ratios, obtained by the integration over a large phase space, such as for the production of $K\pi\pi$ (e.g. $B \to K\pi\pi\gamma\ \psi$) or similar. For instance, Belle [15] defines branching ratios as the ratios of integrals over the whole phase space. If there were not such a cutoff, the higher partial wave contribution such as D-waves would be found much too large with respect to S waves, due to the centrifugal barrier factors k^{2l}, which increase too much at large mass of the $K\pi\pi$ system.[5]

(ii) *Departure of the resonance line shape from the Breit-Wigner formula.* Resonances are usually described by multiplying the standard Breit-Wigner (and the width) by the so-called centrifugal barrier factors. The term is ambiguous, since these factors include both the proper centrifugal barrier effect, which is the universal k^{2l} automatically present in partial waves (increasing with momentum), and the damping factor, which is highly model-dependent and decreases with momentum. In fact the prototype of such factors are the Blatt-Weisskopf factors of nuclear physics, also commonly used by experimentalists in particle physics. They are deduced for a spherical well potential, which is obviously very naive. One consequence of this particular set of factors is that there would be no damping for S waves, which is not true in more realistic models (harmonic oscillator wave functions in the $^3P_0$ model give a Gaussian damping in all waves).
The accurate studies of the resonance shapes show directly a departure from the standard Breit-Wigner shape, e.g. for the $\Delta(1236)$ [31] or the $K^*(890)$, see Ref. [10]).

(iii) *Contribution of loops to self-energy.* The need for the cutoff is also shown by calculations of the

[5]Experimentally, the problem does not appear in the work of the Belle Collaboration [15] because it does not introduce D-waves for the K_1-decays.

hadronic loop contribution to the self-energy of mesons (see Sec. IV A 2), which involves integration over the possible momentum up to infinity. In the $^3P_0$ model [32], the contribution to the self-energy would be much too large for D-waves, in spite of the cutoff naturally provided by the Gaussian wave functions, yielding finally a bad spectrum.

One obtains a natural damping factor through the Gaussian factors $e^{-\beta k^2}$:

$$A_S \propto (3 - \alpha k^2) e^{-\beta k^2}, \qquad A_D \propto \alpha k^2 e^{-\beta k^2}, \tag{14}$$

but one finds $\beta \sim 0.3$ GeV^{-2}, which is much too small; it does not reduce efficiently the D-wave contributions for the loops or the off shell situations we consider. Following Ref. [32], we introduce the empirical Gaussian cutoff $\exp[-\beta'(k^2 - k_0^2)]$ with $\beta' \approx 3$ GeV^{-2}, where k_0 is the decay momentum when all the particles are put on shell:

$$\begin{aligned} A_S &\propto (3 - \alpha k^2) e^{-\beta k^2} \times e^{-\beta'(k^2 - k_0^2)}, \\ A_D &\propto \alpha k^2 e^{-\beta k^2} \times e^{-\beta'(k^2 - k_0^2)}. \end{aligned} \tag{15}$$

With this additional damping factor, one finds that the integrated D/S ratio becomes stable. The isobar (K^*/ρ) decay does not depend much on the damping factor. However, another effect then appears in the decay rate from the parent K_1 to one isobar and one stable particle: Integrating over the mass of the isobar, the calculated partial width depends on the presence of the damping factor for the decay of the parent K_1 resonance to an off shell isobar. The low end of the isobar mass spectrum corresponds indeed to large off shell momenta. This effect has been duly taken into account in our calculations.

In the calculation of λ_γ presented in our previous paper [3], the effect of the introduction of this damping factor in the decay amplitude of the K_1 is important. Indeed, the interference of several channels needed to obtain a nonzero imaginary part of $\vec{n} \cdot (\vec{\mathcal{J}} \times \vec{\mathcal{J}}^*)$ requires a large off shellness of the intermediate isobars. We find that this quantity is sensitive to the presence of the D waves, and then to the introduction of the damping factor.

IV. HOW TO COMPARE THEORETICAL MODEL COMPUTATION WITH EXPERIMENTAL DATA

Let us stress that the use of experimental data in our work is twofold: First determine the model parameters γ and θ_{K_1}, and then check the validity of our model predictions.

In this section, we will explain how one can relate the quark model predictions for the decay partial widths of K_1 to the K-matrix analysis of Daum *et al.* , which is the main source of experimental information.

Indeed, the main experiments on the K_1-decays [7,8] were analyzed with the same K-matrix formalism developed by Bowler *et al.* [33] and obtained very similar results. We use in our analysis the parameters of the analysis done by Daum *et al.* (ACCMOR experiment), which seems to be the most detailed. On the other hand, there are certain physical parameters of the fit which are not tabulated in this paper. Then we also use, where necessary, the results of the K-matrix reanalysis of the ACCMOR data by the *BABAR* Collaboration [16].

Let us now emphasize that the very extensive work of Daum *et al.* consists of two distinct steps:

(i) The first one is the partial wave analysis where the $K\pi\pi$ three-body final state is decomposed into a sum of quasi-two-body partial waves ($K^*\pi$, $K\rho$, etc.) with various quantum numbers of the total spin and orbital momentum. In this first step, there is no reference to any parent resonance like K_1. This step corresponds to the fitted values of the quasi-two-body partial wave amplitudes plotted with the corresponding error bars in Ref. [8].

(ii) The second step is the fit of the partial wave amplitudes, extracted in the previous step, within the K-matrix formalism in order to study the structure of the initial parent K_1 resonance and its properties (pole masses, couplings to various decay channels, etc.).

Let us stress that this two-step procedure is different from the modern Dalitz plot analyses where the isobar and parent resonances are included together in one unique formula of the total amplitude. In that case, the total amplitude is written directly as a product of the parent resonance decay amplitude and the amplitude of the subsequent decay of the isobar, taking into account the width effects of the unstable resonances by the Breit-Wigner forms.

We do not question the first step; we rather indicate various difficulties which we have encountered in trying to use the K-matrix parameters from the analysis of Daum *et al.* . In the following subsection, we first recall the general K-matrix formalism and then its relation to the quark model.

A. K-Matrix Formalism and Quark Model

In order to extract our theoretical parameters, γ and θ_{K_1}, we need the experimental partial widths. We also need them to verify our prediction of the model. And the question is, how to define a partial width? Resonances are often parametrized in terms of the Breit-Wigner form

$$\begin{aligned} \mathrm{BW}_r^{(\mathrm{NR})}(m) &\propto \frac{1}{m_r - m - i\frac{\Gamma_r}{2}}, \quad \text{or} \\ \mathrm{BW}_r^{(R)}(m) &\propto \frac{1}{m_r^2 - m^2 - i m_r \Gamma_r} \end{aligned} \tag{16}$$

in the nonrelativistic and relativistic cases, respectively. Resonance width, in principle, depends on energy, $\Gamma_r(m)$.

This approximation assumes an isolated resonance with a single measured decay. If there is more than one resonance in the same partial wave and they strongly overlap, an elegant way that provides the unitarity of the S-matrix is to use the K-matrix formalism for the two-body decays of the resonance states.[6]

1. General Definitions in K-Matrix Formalism

From the unitarity of the S-matrix

$$S \equiv 1 + 2i\rho^{(1/2)} T \rho^{(1/2)}, \tag{17}$$

one gets

$$T - T^\dagger = 2iT^\dagger \rho T = 2iT\rho T^\dagger, \tag{18}$$

where the diagonal matrix $\rho_{ij}(m)$ is the phase-space factor which is discussed in detail later in this section. In terms of the inverse operators, Eq. (18) can be rewritten as

$$(T^\dagger)^{-1} - T^{-1} = 2i\rho. \tag{19}$$

One can further transform this expression into

$$(T^{-1} + i\rho)^\dagger = T^{-1} + i\rho. \tag{20}$$

Using the definition of the K-matrix

$$K^{-1} \equiv T^{-1} + i\rho, \tag{21}$$

one can easily find from Eqs. (20) and (21) that the K-operator is Hermitian, i.e.

$$K = K^\dagger. \tag{22}$$

From the time reversal invariance of S and T, it follows that K must be symmetric, i.e. the K-matrix can be chosen to be real and symmetric. Resonances should appear as a sum of poles in the K-matrix. In the approximation of resonance dominance, one gets therefore

$$K_{ij} = \sum_{a'} \frac{f_{a'i} f_{a'j}}{m_{a'} - m} \tag{23}$$

where the sum on a' goes over the number of poles with masses $m_{a'}$. In the common approximation in the resonance theory, the couplings $f_{a'i}$ are taken to be real.

The partial and total K-matrix widths can be defined as

$$\Gamma_{a'i}(m) = 2f_{a'i}^2 \rho_{ii}(m) \tag{24a}$$

$$\Gamma_{a'}(m) = \sum_i \Gamma_{a'i}(m). \tag{24b}$$

Note that the K-matrix width does not need to be identical to the width, which is observed in experiment, nor to the width of the T-matrix pole in the complex energy plane.

2. Relation Between Couplings in K-Matrix Formalism and Quark Model

In this section, we identify in a systematic approach the couplings deduced from the $^3P_0$ quark model, including the mixing of K_1 resonances, with the couplings introduced in the K-matrix formalism by Bowler *et al.* [33]. To justify this identification, we establish the connection between the formalism introduced in the previous section and the quark model.

(1) To make explicit the discussion in Ref. [34], we distinguish two types of interactions:

(i) The first type of interaction is described by Hamiltonian H_0, which describes the $q\bar{q}$ potential of the bound states of mesons, $\{a^0, b^0, \ldots\}$. It generates the initial meson masses and wave functions which are used to calculate the matrix elements of meson decays in the quark model (see next item).

(ii) The second type of interaction, described by Hamiltonian H', represents the interaction vertices connecting these bound states to the continuum of all possible states of two interacting mesons, $\{i, j, \ldots\}$:

$$f_{a^0 i} = \langle a^0 | H' | i \rangle \tag{25}$$

We commonly call these vertex interactions "couplings." These couplings can be precisely calculated within the $^3P_0$ quark-pair-creation model. With adequate choice of phases of the wave functions of the bound states, the couplings can be set to be real.

(2) No direct interaction is assumed between two mesons. Nevertheless, there is rescattering, since a meson pair can annihilate into one bound state and then be created again from the decay of this bound state. This rescattering process can be iterated an arbitrary number of times, equivalent to a resummation of meson loops between the initial and final vertices (see Fig. 2).

All these possible processes can be resummed into a matrix propagator $\Pi_{a^0 b^0}$ connecting two vertices. Let us call the scattering energy m. The couplings can be in principle energy-dependent, i.e., be a function of m. This is the case with centrifugal barrier or damping factors, which are indeed present in our model. However, for simplicity of presentation we assume them to be constant. Then, defining the "bare" scattering amplitude for the first diagram in Fig. 2 ,

$$T_{ij}^{a^0(0)} = \frac{f_{ia^0} f_{a^0 j}}{m_{a^0} - m} \tag{26}$$

[6]Note that in the case of two overlapping resonances the Breit-Wigner parametrization of the amplitude satisfies the unitarity condition of the S-matrix only with the complex couplings satisfying certain conditions. As we will demonstrate, these complex couplings can be obtained from the real K-matrix couplings by a complex rotation.

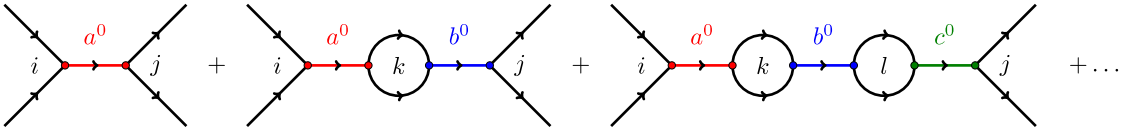

FIG. 2 (color online). Rescattering process.

and resumming all possible diagrams with leads to the scattering amplitude

$$T_{ij} = \sum_{a^0} T_{ij}^{a^0(0)} + \sum_{a^0,k,b^0} T_{ik}^{a^0(0)} I_k T_{kj}^{b^0(0)} + \sum_{a^0,k,b^0,l,c^0} T_{ik}^{a^0(0)} I_k T_{kl}^{b^0(0)} I_l T_{lj}^{c^0(0)} + \ldots = \sum_{a^0,b^0} f_{ia^0} \Pi_{a^0 b^0} f_{b^0 j} \quad (27)$$

where the propagator defined as

$$\Pi_{a^0 b^0}(m) = \frac{\delta_{a^0 b^0}}{m_{a^0} - m} + \frac{f_{a^0 k} f_{k b^0}}{(m_{a^0} - m)(m_{b^0} - m)} I_k + \ldots = \left(M(m) - i\frac{\Gamma(m)}{2} - m \right)^{-1}_{a^0 b^0}, \quad (28)$$

with I_k being the loop integral for the rescattering loop of the kth channel. In the case where the couplings f depend actually on m, one should include the coupling factors relative to the internal lines of Fig. 2 in the loop integral. However, since we do not attempt actually to calculate the loops, we see that there is no need to introduce this complication.

The mass matrix in Eq. (28) is:

$$\left(M - i\frac{\Gamma}{2} \right)_{a^0 b^0} = m_{a^0} \delta_{a^0 b^0} - \sum_i f_{ia^0} f_{b^0 i} I_i. \quad (29)$$

It is in general nondiagonal. It contains

(i) the initial diagonal mass matrix diag$(m_{a^0}, m_{b^0}, \ldots)$ of the bound states;

(ii) the contribution of the loops for each possible channel, which can be nondiagonal since common two-body channels can couple to two different bound states. The loop integrals contain real and imaginary parts, which appear only when a two-body channel is open at the energy m.

(3) Now the mass matrix must be diagonalized in two steps as explained in Ref. [34]. One first diagonalizes the real part, M, then one passes to a diagonalization of the full new matrix, $M' - i\Gamma'/2$.

(a) Diagonalization of the real part of the denominator of $\Pi_{a^0 b^0}$ matrix, M, leads to the introduction of the new diagonal mass matrix

$$M'(m) = \text{diag}(m_{a'}, m_{b'}, \ldots). \quad (30)$$

This mass diagonalization implies a simultaneous rotation of the couplings $\{f_{a^0 i}\}$, leading to the new couplings $\{f_{a' i}\}$. One thus passes to the masses and couplings of the K-matrix, Eq. (23). Of course, if there exists only one resonance which couples to the initial and final states, no rotation is needed. In this case, all bare couplings $\{f_{a^0 i}\}$ coincide with the ones of the K-matrix, $\{f_{a' i}\}$. Thus, one can relate them with couplings calculated in the quark model. Otherwise, when there are two possible overlapping resonances, namely, the two K_1s, we have to make a rotation and introduce a mixing angle. We notice then that we have introduced an arbitrary rotation angle θ_{K_1} in our model computations, which allows us to identify the set of the observed K-matrix couplings with the theoretical ones by the fit of data with our model predictions. This identification means that:

(i) the effect of the real part of the loops, i.e. Re(I_k) in Eq. (27), is taken into account in our model;

(ii) mixing angle θ_{K_1} is not predicted by the model but is simply adjusted to data;

(iii) introduction of the mixing angle θ_{K_1} can also take into account the uncalculated rotation of the pure spin states K_{1A} and K_{1B} into the eigenstates of Hamiltonian H_0 due to the spin-orbit forces [35].

(b) The second step consists the diagonalization of the new mass matrix

$$\left(M' - i\frac{\Gamma'}{2} \right)_{a' b'} = m_{a'} \delta_{a' b'} - i \sum_i \rho_{ii}(m) f_{a' i} f_{i b'}. \quad (31)$$

This leads to the physical mass eigenstates and to the Breit-Wigner parametrization with energy-dependent width. This new rotation that accomplishes the last transformation into the physical states must have a complex and the angle of this rotation must have a complex phase. This would lead to the complex couplings of the mass eigenstates to a set of continuum states (see Fig. 9). As we have already mentioned in the text, this rotation seems to be rather small.

(4) Let us now discuss the dependence of various variables on the energy m. In principle, all the masses and couplings produced by the two previous steps are dependent on m because of the loop effects (the bare couplings themselves may depend on m, as is

the case of our quark model, when one calculates the decay momenta, then the widths at the mass m. This then modifies the expression of the loop integral). This also implies that the real mixing angle θ_{K_1} is also energy-dependent in principle. However, as regards the mass matrix, its real and imaginary parts have rather different behavior depending on m. In the first approximation, the real part of the mass matrix, which includes the sum of the large number of loops, varies slowly with m and can be considered as constants on a limited range of energy. This is what was done in the analysis of Daum *et al.* . On the contrary, the imaginary part, which corresponds to the partial widths of the opened channels, is a rapidly varying function near the threshold.

One can go beyond the approximation of the real part of the mass matrix by taking into account that there is some variation near the threshold. This is obtained by analytic continuation of the phase space through the threshold. This effect is consistently included in the prescription of Nauenberg and Pais of the complex phase space, although we differ on other assumptions they made. This corresponds to having imaginary part of the widths generating a m-dependent mass shift. For instance, for the K-matrix width one have

$$\Gamma_{a'b'}(m) = \sum_i \rho_{ii}(m) f_{a'i} f_{ib'} \tag{32}$$

where the phase-space factor $\rho_{ij}(m)$ can be complex in general.

Finally, one obtains for the physical states that the physical masses of $K_1(1270/1400)$ are varying slowly as functions of m while the physical widths are rapidly changing functions; moreover, the mass of $K_1(1270)$ has a more rapid variation around the peak due to the closeness of the K_1-mass to the $K\rho$ threshold (see Fig. 10).

In summary, one should identify the K-matrix couplings with the ones predicted in the $^3P_0$ model, with the real mixing effect included to define the initial states in this model. To establish the quantitative relation between the definitions in these two formalisms, we identify more exactly the partial widths, $\Gamma^{\mathrm{QPCM}}_{K_1 i}(M_{\mathrm{peak}})$:

$$\Gamma^{\mathrm{QPCM}}_{K_1 i}(M_{\mathrm{peak}}) = \Gamma_{K_1 i} = 2 f^2_{K_1 i} Re[\rho_{ii}(M_{\mathrm{peak}})], \tag{33}$$

where $\Gamma^{\mathrm{QPCM}}_{K_1 i}(M_{\mathrm{peak}})$ is the $^3P_0$ model partial width, Eq. (10); $\Gamma_{K_1 i}$, ρ_{ij} and $f_{K_1 i}$ are, respectively, the partial width, the phase space (we use the real part of the phase space since ρ_{ij} is defined as a complex quantity, as will be explained later), and the K-matrix couplings in the formalism of Daum *et al.* . Note that these are not exactly the common partial widths related to the Breit-Wigner analysis; the latter would be obtained by applying the complex rotation [see Eq. (31)].

Now, Eq. (10) is valid only for the narrow isobar. If we have to take into account the effect of the finite width of the isobar, we have to integrate the quasi-two-body phase space over the Breit-Wigner of the isobar. One has to underline that in this approach we do not have to integrate over the Breit-Wigner of the K_1-resonance, unlike what is done, for instance, in Ref. [28]. We indeed calculate the width at the peak. On the contrary, if we would like to compare with the results of the Belle Collaboration analysis [15], this approach must be changed, and we would have to integrate over the whole three-body phase space of $B \to K\pi\pi\psi$ to obtain the branching ratios. But even in that case, it does not make sense, in our opinion, to integrate the decay widths themselves over the Breit-Wigner of the K_1.

B. Observed Problems in Experimental K-Matrix Analysis

As announced, we found several problems in using the experimental analysis:

(1) Absence of the $K\pi\pi$ nonresonant contribution in the K-matrix

We note that the K-matrix of Daum *et al.* is composed only of two resonance poles. There is no nonresonant contribution which is usually parametrized as polynomial in terms of m in the K-matrix parametrization. This implies the strong assumption that the quasi-two-body scattering of vector-scalar mesons ($K^*\pi$ and $K\rho$) passes only through the K_1 resonant intermediate states.

(2) D-wave amplitudes issue

The results of the ACCMOR analysis [8] show that the D-wave in $K_1(1270) \to K^*\pi$ depends strongly on the production transfer t in the $Kp \to K\pi\pi p$ reaction. This fact may escape the attention of PDG reader, because it averages between two sets of data (low t, high t). As for the D-wave amplitude in the $K\rho$ channel, there is no information; only branching ratios are quoted in the paper but not the K-matrix couplings and their phases which are crucial for our study.

(3) The problem of definition of the total width with threshold effect

When the mass of the resonance at the peak is close to a decay threshold, different definitions of the resonance width are no longer equivalent. Such possible definitions are the width at the peak $\Gamma(M_{\mathrm{peak}})$, the width at the S-matrix pole, and finally the full width if measured at one-half the maximum height of the Breit-Wigner distribution, defined as

$$\Gamma^{\mathrm{FWHH}}_{K_1} \equiv m_2 - m_1, \tag{34}$$

TABLE III. Experimental total decay widths, calculated using the fitted parameters from Ref. [8]. In our opinion, only the widths calculated at the peak must be used to compute partial widths from the branching ratios. Note that the D-waves are not included in the $\Gamma_{K_1}^{\text{peak}}$ estimation.

K_1	$\Gamma_{K_1}^{\text{ACCMOR}}$, MeV/$c^2$	$\Gamma_{K_1}^{\text{peak}}$, MeV/$c^2$	$\Gamma_{K_1}^{\text{FWHH}}$, MeV/$c^2$
$K_1(1270)$	90 ± 8	~ 190	~ 80
$K_1(1400)$	165 ± 35	~ 230	~ 230

where m_1 and m_2 are defined as two solutions in m of the equation

$$\frac{f_{a'(b')1}^2 \rho_{11}(m)}{m_{a'(b')} - m - i\Gamma_{a'(b')}(m)} = \frac{1}{2} \frac{f_{a'(b')1}^2 \rho_{11}(M_{\text{peak}})}{m_{a'(b')} - M_{\text{peak}} - i\Gamma_{a'(b')}(M_{\text{peak}})} \tag{35}$$

using the $K^*\pi$ channel (labeled as channel 1).

The last two widths are found to be smaller than the first one. That is why the $K_1(1270)$ width, $\Gamma_{K_1(1270)} = (90 \pm 8)$ MeV/c^2 [8], which is assumed to be defined as the full width if measured at one-half the maximum height of the Breit-Wigner distribution of K_1, is less by a factor 1.5–2 than the total width at the peak (see Table III), which is computed using the K-matrix couplings and summing over all possible intermediate channels, i.e.

$$\Gamma_{K_1}^{\text{peak}} \equiv 2 \sum_i f_{K_1 i}^2 \text{Re}[\rho_{ii}(M_{\text{peak}})] \tag{36}$$

We find, indeed, for the latter to be of the order of 200 MeV/c^2 with the inclusion of the $\kappa\pi$ channel (see Table III). As a consequence, one observes a large discrepancy between the two possible definitions of the partial width that can be extracted from data of the ACCMOR Collaboration: [8] The partial width, defined in a ''standard'' way as $\Gamma(K_1(1270) \to K\rho) = \Gamma_{K_1} \times \mathcal{B}(K_1(1270) \to K\rho)$, is less by a factor of 2–3 compared to the partial width at the peak, defined from the K-matrix couplings (see Table IV). The total width, defined by the ACCMOR Collaboration and tabulated in PDG, seems therefore to be misleading. It should not be used to compare with the quark model predictions. According to us, previous theoretical analyses (for instance, in Ref. [21]) unduly used for experimental partial widths the product of branching ratios with this total width of $K_1(1270)$ quoted by PDG.

(4) The problem of the phase space, ρ_{ij}

In the expression of the T-matrix in the K-matrix formalism, the phase space factor ρ_{ij} is defined as

$$\rho_{ij}(m) = \frac{2k_i(m)}{m} \delta_{ij} \tag{37}$$

Naively, k_i is the breakup momentum for the two-body decay channel i. But in fact, Bowler *et al.* used for k_i a particular formulation, proposed by Nauenberg and Pais [36], which tries to take into account two important effects:

(a) The requirement of the analiticity of the amplitude. The simplest way to satisfy it is the analytic continuation of the phase space through the threshold:

$$\rho_{ij}(m) = \begin{cases} \frac{2k_i(m)}{m} \delta_{ij}, & \text{above threshold} \\ \frac{2i|k_i(m)|}{m} \delta_{ij}, & \text{below threshold} \end{cases} \tag{38}$$

It is the basic idea of the so-called Flatte model, which has been used to analyze the $a_0(980)$-decay into $\eta\pi$ and $K\bar{K}$ states, the resonance being very close to the $K\bar{K}$ decay threshold. Similarly, this effect is also present in the $K_1(1270)$-decays into $K\rho$ and $K^*\pi$ channels with the resonance being at the threshold of $K\rho$. This is not so relevant for the $K_1(1400)$-decays where the resonance is far above the thresholds.

(b) The effect of the isobar width. The peculiarity of the $K_1(1270)$ with respect to the $a_0(980)$ case is that the two-body final state includes one unstable particle, the isobar V ($V = \rho$ or K^*). To take into account the width of the isobar, it is logical to integrate the three-body phase space over the Breit-Wigner of the isobar:

TABLE IV. Experimental partial decay widths, calculated using the fitted parameters from Ref. [8]. As was underlined previously, only the values from the last column must be used.

Decay channel i	$\Gamma_{K_1 i} = \mathcal{B}_{K_1 i} \times \Gamma_{K_1}^{\text{ACCMOR}}$, MeV/$c^2$	$\Gamma_{K_1 i}^{\text{peak}} = 2 f_{K_1 i}^2 \text{Re}\rho_{ii}$, MeV/$c^2$
$K_1(1270) \to (K^*\pi)_S$	12 ± 3	28 ± 26
$K_1(1270) \to (K\rho)_S$	41 ± 10	122 ± 28
$K_1(1400) \to (K^*\pi)_S$	162 ± 13	211 ± 59
$K_1(1400) \to (K\rho)_S$	2 ± 2	20 ± 25

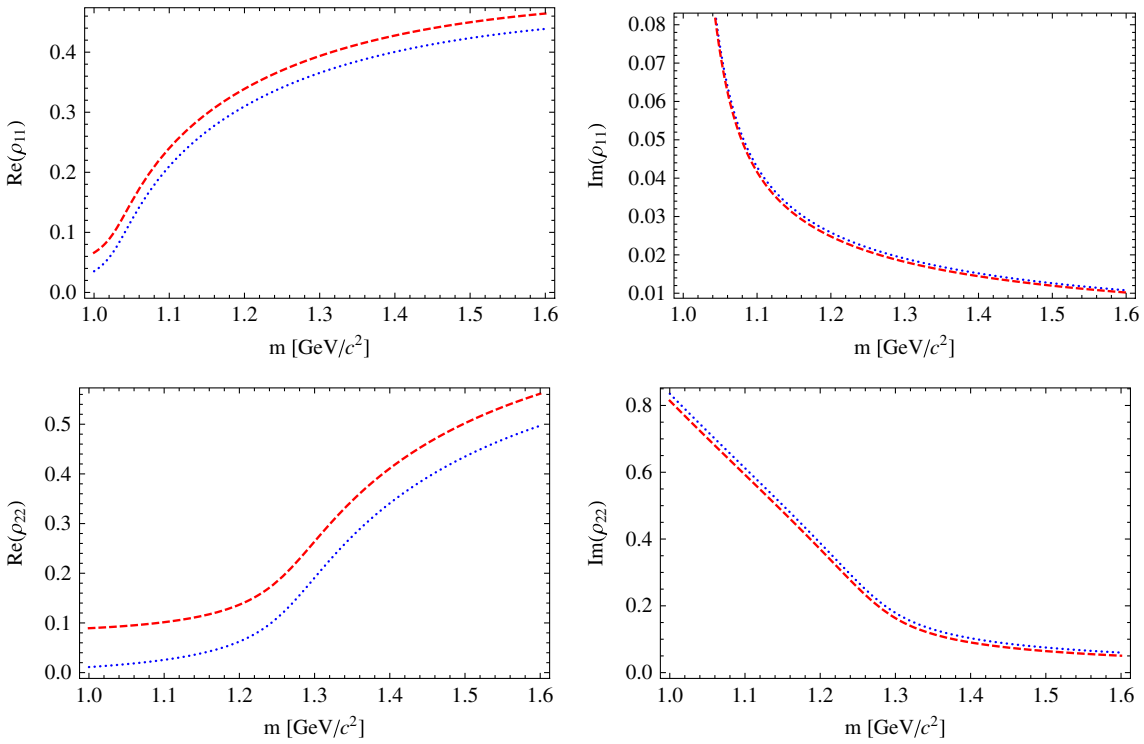

FIG. 3 (color online). Dependence of the phase space factor ρ_{ij} on the mass of the decaying resonance m for the $K^*\pi$ (top) and $K\rho$ (bottom) channels. For comparison, ρ_{ij} is calculated using the proper analytic continuation, Eq. (39), (dotted lines) and the approximation of Nauenberg and Pais, [36] Eq. (41), (dashed lines). The difference between two approaches for Re(ρ_{22}) turns out to be significant for the $K\rho$ channel.

$$k_i(m) = \int_{m_V^{\min}}^{\infty} k_i(m, m_V) \frac{\Gamma_V/2\pi}{(M_V - m_V)^2 + \frac{\Gamma_V^2}{4}} dm_V, \tag{39}$$

where $k_i(m, m_V)$ has its nonrelativistic expression[7]

$$k_i(m, m_V) = \sqrt{\frac{2m_V m_P}{m_V + m_P}(m - m_V - m_P)} \tag{40}$$

The infinite upper limit in Eq. (39) corresponds to the analytical continuation of k_i below the threshold for $m_V > m - m_P$.

As an approximation to this integral, Nauenberg and Pais [36] proposed to use the complex mass of the isobar, $M_V \to M_V - i\Gamma_V/2$, in the expression of the momentum $k_i(m, m_V)$. These two prescriptions lead to a complex phase space, defined as

$$\rho_{ij}(m) = \frac{2k_i(m)}{m}\delta_{ij} = \frac{2}{m}\sqrt{\frac{2M_V m_P}{M_V + m_P}\left(m - M_V - m_P + i\frac{\Gamma_V}{2}\right)_i}\delta_{ij}, \tag{41}$$

where P ($P = K$ or π) is the final state pseudoscalar meson in the quasi-two-body decay. According to us, this prescription of using a complex mass is not satisfactory for the ρ and K^*, especially for $K_1(1270) \to K\rho$. Indeed, we found by direct integration of Eq. (39) that the results are quite different from the ones obtained using Eq. (41), especially the real part of $\rho_{ij}(m)$ which corresponds to the real phase space in the $K_1(1270) \to K\rho$ case (see Fig. 3). The same observation was formulated by Frazer and Hendry [37] when the paper of Nauenberg and Pais was published. They pointed out that this approximation is valid only for the very narrow resonances. The failure of this approach is very worrying since it is basic for the whole analysis of Daum *et al.* . In order to cure this problem, we formulate the following assumption: As we will explain, instead of identifying the K-matrix couplings themselves, we assume that it

[7]For the relativistic phase space, Eq. (27) no longer defines a real K-matrix in the physical region. The reason is that the relativistic momentum does not remain imaginary below the threshold due to an additional complex branch point $\propto \sqrt{m^2 - (m_V - m_P)^2}$. Therefore, Nauenberg and Pais in Ref. [36] restricted to nonrelativistic case.

is the product of the couplings squared and the phase space which is given in a correct way by the experiment, at least approximately.

(5) The problem of the P- and D-waves
In addition, the prescription of Nauenberg and Pais has not been established for the P- and D-waves. We do not know what has been done exactly by Daum *et al.* to treat these waves. On the other hand, such waves are to be included in the analysis; the $\kappa\pi$ in the P-wave is especially important. Since we are not able to redo the analysis by Daum *et al.*, we use the couplings to $K_0^*(1430)\pi$ channel refitted by the *BABAR* Collaboration [16]. They include a centrifugal barrier factor depending on the complex momentum, which is defined by Eq. (41).[8] However, there is a new following problem here. The approximation of *BABAR* for the centrifugal barrier factor is not an approximation to the integral

$$\int_{m_V^{\min}}^{\infty} k_i(m, m_V)\left[\frac{k_i^2(m, m_V)\tilde{R}^2}{1 + k_i^2(m, m_V)\tilde{R}^2}\right] \times \frac{\Gamma_V/2\pi}{(M_V - m_V)^2 + \frac{\Gamma_V^2}{4}} dm_V, \tag{42}$$

which gives a positive real part while the approximation gives a negative one. This contradiction can be masked by the normalization of the centrifugal barrier factor at the peak. However, this is obviously not a satisfactory solution.

(6) The diagonalization of the mass matrix and corresponding rotation of the K-matrix couplings into physical couplings
In several cases, we have to deal not with the K-matrix couplings but with Breit-Wigner parametrization of the intermediate resonances. This is the case, for example, in our calculation of the $\mathcal{J}$-function. This is also the case of the Dalitz plot analyses, such as the one of the Belle Collaboration [15]. Then the relevant couplings are slightly different from those of the K-matrix. As stated previously, they are obtained from the latter by a complex rotation. Indeed, to pass to the physical states, we have to diagonalize the mass matrix of the states in the K-matrix formalism. This diagonalization can be performed by a complex orthogonal matrix. This rotation is complex because of the nondiagonal elements of the imaginary part of the mass matrix. The complex rotation angle (which depends on the energy) has both real and imaginary parts, which are found to be of the order 10° (this result was obtained by explicit diagonalization of the mass matrix). As a consequence, this rotation affects the couplings: The rotation makes the couplings of the Breit-Wigner somewhat different from the ones of the real K-matrix. The magnitudes of the new couplings are different and phases appear. We found that the largest couplings (i.e. considering the dominant decay channels, $K_1(1270) \to K\rho$ and $K_1(1400) \to K^*\pi$) are slightly affected and acquire small phases. On the other hand, for the smallest couplings ($K_1(1270) \to K^*\pi$ and $K_1(1400) \to K\rho$), the rotation effects are more important. In practical calculations of λ_γ for the present moment we have neglected these effects so that we use directly the couplings obtained from the $^3P_0$ mode.[9]

(7) Relative signs and offset phases.
It appears that the phases of the amplitudes, deduced from the experimental K-matrix analysis, are not exactly what is observed: This is a phenomenon of so-called offset phases. The $K\rho$ channel was found to have an additional unexplained phase of 30° [8] relative to the $(K^*\pi)_S$, which was set as a reference one. For the $\kappa\pi$ channel, the discrepancy reaches 90°.
Another problem is that we are not able to establish the complete relation between the phase conventions of Daum *et al.* and quark model ones, since the paper of the ACCMOR Collaboration is not detailed enough.

V. NUMERICAL RESULTS

Let us summarize our final prescriptions we use for the calculation of the partial widths and for the further extraction of our theoretical model parameters from the experimental measurements. Our basic approach is to use partial widths at the peak on both theoretical and experimental sides. We abandon the idea of using the branching fractions and the total K_1-widths for the comparison with our predictions.

(1) For the theoretical prediction, in order to take into account the isobar width effects in our theoretical prediction of the partial widths $\Gamma_{K_1 i}^{\mathrm{QPCM}}$, the amplitudes (9) squared are integrated over the invariant mass of the isobar:

$$\Gamma_{K_1 i}^{\mathrm{QPCM}} = 8\pi^2 \int_{m_V^{\min}}^{M_{K_1} - m_P} \frac{E_V E_P k_P}{M_{K_1}} |A_i(K_1 \to VP)|^2 \times \frac{\Gamma_V/2\pi}{(M_V - m_V)^2 + \frac{\Gamma_V^2}{4}} dm_V. \tag{43}$$

Note that since we consider the widths at the peak, there is no integration over the K_1 invariant mass, unlike what is done in several theoretical papers (e.g., see Ref. [28]). Moreover, one can notice that the integration over the mass of the isobar is one

[8] According to private communications.

[9] For more details, see Appendix A.

within the correct physical region restricted by the corresponding physical bound of the two-body decay (i.e., we use the real phase space).

(2) For the experimental input, we make the simple assumption that the partial widths, calculated from the K-matrix couplings at the peak according to Eq. (44), are correct, although the complex phase space *à la* Nauenberg and Pais (41) might be not correct (i.e., what we measure by fitting data is always the combination like $f^2_{a'(b')i} \times \rho_{ij}(m)$, which are assumed to be extracted correctly). Therefore, we use the K-matrix couplings and the real part of the complex phase space *à la* Nauenberg and Pais in order to extract the experimental values of the partial widths

$$\Gamma^{\text{peak}}_{K_1 i} = 2 f^2_{a'(b')i} \text{Re}[\rho_{ij}(M_{\text{peak}})]. \tag{44}$$

(3) We calculate this partial width according to Eq. (24) also for the P- ($L = 1$) and D-waves ($L = 2$), assuming that the K-matrix couplings f contain the barrier factors $B^L_i(m)$ that are properly normalized at the peak:

$$\begin{aligned} f_{a(b)i}(m)|_{P,D-\text{waves}} &= f_{a(b)i} \frac{B^L_i(m)}{B^L_i(M_{\text{peak}})} \\ B^L_i(m) &= \left[\frac{k^2_i(m)\tilde{R}^2}{1 + k^2_i(m)\tilde{R}^2}\right]^{L/2}, \end{aligned} \tag{45}$$

where $\tilde{R}^2 = 25\ \text{GeV}^{-2}$ [16]. This assumption seems to be correct since it leads to the calculated branching ratios that are very close to the ones announced in the paper by Daum *et al.* . In any case, we avoid as much as possible relying on the experimental data on $K_1(1270) \to K\rho$ and the D-wave of $K_1(1270) \to K^*\pi$, and we trust our theoretical prediction.

A. Fit of Parameters γ and θ_{K_1}

In order to extract our phenomenological parameters, the quark-pair-creation constant γ and K_1 mixing angle, we do a fit using the method of least squares. As an experimental input, we use the partial widths (namely $\Gamma^{\text{peak}}_{K_1 i}$ from Table IV) only from the following processes: $K_1(1270) \to (K^*\pi)_S$, $K_1(1400) \to (K^*\pi)_S$, and $K_1(1400) \to (K\rho)_S$, which are assumed to be Gaussian distributed with mean $\Gamma^{\text{QPCM}}_{K_1 i}(\gamma, \theta_{K_1})$ and known variance $\sigma_{\Gamma^{\text{peak}}_{K_1 i}}$. The D-waves are not taken into account in our fit. Moreover, the dominant channel $K_1(1270) \to K\rho$, due to the dangerous threshold and phase space effects, is avoided, since the narrow width approximation can be incorrect for the decays near the threshold and here the width effects can play a significant role.

Then, the likelihood function is constructed as a sum of squares

$$\begin{aligned} \chi^2(\gamma, \theta_{K_1}) &= -2 \ln L(\gamma, \theta_{K_1}) \\ &= \sum_{i=1}^{3} \frac{(\Gamma^{\text{peak}}_{K_1 i} - \Gamma^{\text{QPCM}}_{K_1 i}(\gamma, \theta_{K_1}))^2}{\sigma^2_{\Gamma^{\text{peak}}_{K_1 i}}} \end{aligned} \tag{46}$$

In order to find the unknown parameter θ_{K_1}, the function χ^2 is minimized, or equivalently the likelihood function $L(\theta_{K_1})$ is maximized. The minimization of the χ^2 gives the minimal value $\chi^2_{\text{min}} = 0.61$ and the estimators $\hat{\gamma} = 4.0$ and $\hat{\theta}_{K_1} = 59°$.

The covariance matrix for the estimators $\mathcal{V}_{ij} = \text{cov}[\hat{\xi}_i, \hat{\xi}_j]$ can be found from

$$(\mathcal{V}^{-1})_{ij} = \frac{1}{2} \frac{\partial^2 \chi^2}{\partial \xi_i \partial \xi_j} \bigg|_{\xi = \hat{\xi}}. \tag{47}$$

Thus one obtains

$$\text{cov}[\hat{\gamma}, \hat{\theta}_{K_1}] = \begin{pmatrix} \sigma^2_{\gamma} & C_{\gamma\theta_{K_1}} \\ C_{\gamma\theta_{K_1}} & \sigma^2_{\theta_{K_1}} \end{pmatrix} = \begin{pmatrix} 0.29 & 0.99 \\ 0.99 & 107.0 \end{pmatrix} \tag{48}$$

where the diagonal elements give the variances $\sigma^2_{\hat{\gamma}}$ and $\sigma^2_{\hat{\theta}_{K_1}}$. Finally, one finds the fitted values of the quark-pair-creation constant and K_1 mixing angle:

$$\gamma \simeq 4.0 \pm 0.5, \qquad \theta_{K_1} \simeq (59 \pm 10)° \tag{49}$$

Assuming that our theory is correct, one is now interested in the quality of the agreement between data and various realizations of the theory, determined by the set of parameters, namely $\{\gamma, \theta_{K_1}\}$. For metrological purposes, one should attempt to estimate as best as possible the complete set of parameters $\{\gamma, \theta_{K_1}\}$. In this case, we use the offset-corrected χ^2 [38]:

$$\Delta\chi^2(\gamma, \theta_{K_1}) = \chi^2(\gamma, \theta_{K_1}) - \chi^2_{\text{min}}, \tag{50}$$

where χ^2_{min} is the absolute minimum value of the χ^2 function of Eq. (46) which is obtained when leaving our model parameters free to vary. The minimum value of $\Delta\chi^2$ is 0 by construction. Here one has to notice that this absolute minimum does not correspond to a unique choice of the model parameters. This is due to the fact that the theoretical predictions used in the analysis are affected by important theoretical systematical errors. Since these systematics are restricted in the allowed regions, there is always a multidimensional degeneracy for any value of χ^2. However, since in our analysis there are only two model parameters, our predictions for $\{\gamma, \theta_{K_1}\}$ are not affected by any other theoretical predictions.

A necessary condition that the confidence level (CL) constructed from $\Delta\chi^2(\gamma, \theta_{K_1})$ provides correct coverage is

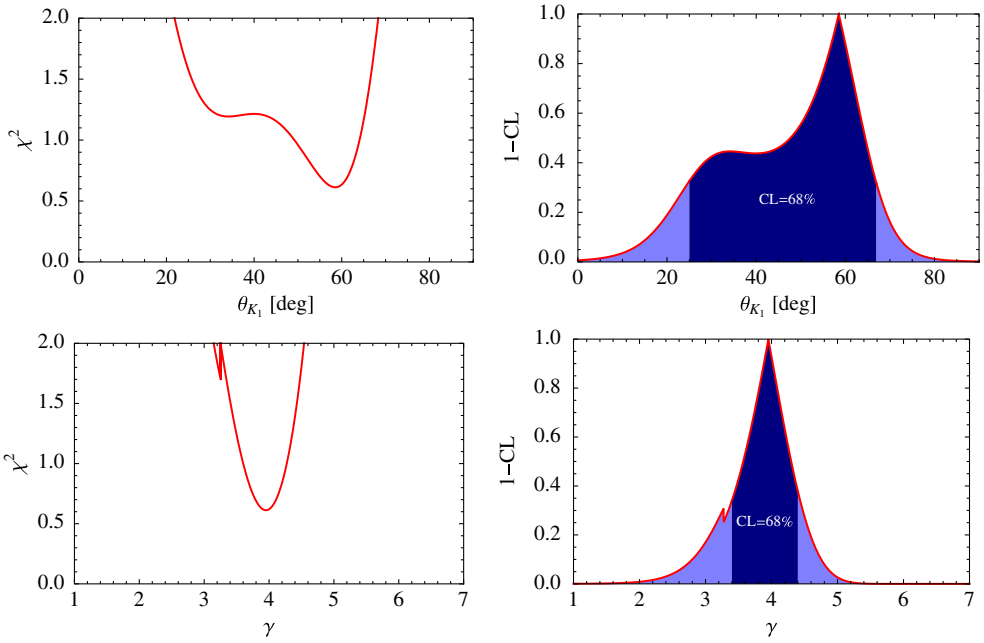

FIG. 4 (color online). χ^2 distributions for the fitted parameters, K_1 mixing angle θ_{K_1} and quark-pair-creation constant γ (left), with the confidence level intervals that determine how frequently the observed interval contains the parameters (right).

that the CL interval[10] for $\{\gamma, \theta_{K_1}\}$ covers the true parameter value with a frequency of 1-CL if the measurements were repeated many times. The corresponding CL intervals for the confidence level of CL = 68% are shown in Fig. 4.

B. Model Predictions for Partial Widths

Now we can make systematic predictions for various processes. First, it is very useful to check our result for the quark-pair-creation constant γ prediction with the much better-studied $b_1 \to (\omega\pi)_S$ and $b_1 \to (\omega\pi)_D$ decays,[11] which depend only on γ. One can see from Fig. 5 that our estimation for γ, determined from the K_1-decays (49), is in good agreement with the one extracted from the $b_1 \to \omega\pi$ decay. Moreover, the extracted D/S ratio of the partial amplitudes is very well predicted and coincides with the measured value, including the sign

$$(A_D/A_S)_{\mathrm{QPCM}} \simeq 0.28, \tag{51}$$

while the experiment [39] gives:

$$(A_D/A_S)_{\mathrm{exp}} = 0.277 \pm 0.027. \tag{52}$$

Note that the Belle Collaboration [15] omits the D-waves in the $B \to J/\psi K_1$ analysis. This could be of consequence, since the Dalitz plot should be appreciably different according to our calculation (see our discussion at the end of Sec. V C 3)

To summarize, we give in Table V our predictions for the S-wave partial widths of the strong interaction decays of the K_1-mesons, using the fitted values of γ and θ_{K_1}. One

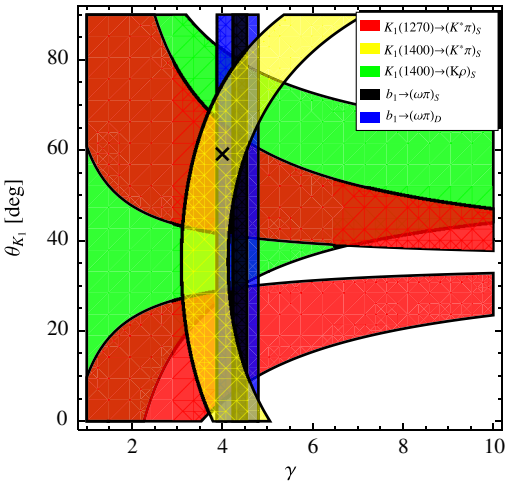

FIG. 5 (color online). QPCM constraints for the quark-pair-creation constant γ and the K_1 mixing angle θ_{K_1} obtained from the fitted partial decay widths at the peak, calculated using the K-matrix couplings (Table IV). The cross indicates the optimal values of γ and θ_{K_1} extracted from the fit.

[10] In statistics, a confidence level interval is a particular kind of interval estimate of a fitted parameter and is used to indicate the reliability of an estimate. It is an observed interval (i.e., it is calculated from the observations), in principle different from sample to sample, that frequently includes the parameter of interest if the experiment is repeated. How frequently the observed interval contains the parameter is determined by the confidence level.

[11] One has to point out that the branching ratio of $b_1 \to \omega\pi$ has not been measured precisely. However, the $\omega\pi$ is considered to be the dominant decay mode [39], so that we assume $\mathcal{B}(b_1 \to \omega\pi) \simeq 100\%$.

TABLE V. Theoretical predictions for the partial decay widths, calculated using the fitted parameters $\gamma = 4.0$ and $\theta_{K_1} = 59°$ and compared to the experimental partial values of widths at the peak (see Table IV).

Decay channel i	$\Gamma^{\mathrm{QPCM}}_{K_1 i}$, MeV/$c^2$	$\Gamma^{\mathrm{peak}}_{K_1 i}$, MeV/$c^2$
$K_1(1270) \to (K^*\pi)_S$	31	28 ± 26
$K_1(1270) \to (K\rho)_S$	61	122 ± 28
$K_1(1400) \to (K^*\pi)_S$	209	211 ± 59
$K_1(1400) \to (K\rho)_S$	1	20 ± 25

can see that the agreement is satisfactory except for the $K_1(1270) \to K\rho$ channel. This is not unexpected in view of the particular difficulties of the experimental treatment in this decay, as explained in the previous section (recall especially that the drawback of using the phase space formula of Nauenberg and Pais [36] is crucial in this case).

As for the D-waves in the K_1-decays, our impression is that they are poorly determined experimentally. Our prediction ($\Gamma(K_1(1270) \to (K^*\pi)_D) \simeq 3$ MeV/c^2) lies below the experimental numbers: The couplings for the D-waves are not given in the paper by Daum *et al.* . Tentatively, they were refitted by the *BABAR* Collaboration, [16] from which we deduce the partial width $\Gamma(K_1(1270) \to (K^*\pi)_D) = (34 \pm 3)$ MeV/c^2. Here one has to notice that the errors of the refitted parameters are surprisingly small, as the ones obtained by Daum *et al.* .

C. Prediction of Signs of Decay Amplitudes and Offset Phase Issue

Let us recall that, at least for the determination of the photon polarization parameter λ_γ as described in our paper [3], that our goal is to calculate the $\mathcal{J}$-function Eq. (1), which describes the full three-body $K_1 \to K\pi\pi$ decay. As explained, we need in fact the expression $\mathrm{Im}[\vec{n} \cdot (\vec{\mathcal{J}} \times \vec{\mathcal{J}}^*)]$, which depends crucially on the relative phases of the $V \to PP$ couplings and the $K_1 \to VP$ form factors (see Eqs. (22)–(27) in Ref. [3] for the definition). These quantities are directly related to the two-body decay amplitudes, calculated by using the quark model. The phases of these amplitudes do not make sense by themselves, but only in the product of two amplitudes of the subsequent processes which describe the final three-body decay $K_1 \to K\pi\pi$. Then, the relative signs are observable quantities that can also be determined from any careful experimental study of the K_1 decays. We define the relative phases for two $K_1 \to K\pi\pi$ amplitudes of various partial waves via different intermediate isobar states (i.e. $(K^*\pi)_S$, $(K^*\pi)_D$, $(K\rho)_S$). Standardly, the reference partial wave is chosen to be the S-wave of $K^*\pi$. For instance, the relative phase of the $K_1 \to K\rho \to K\pi\pi$ channel is defined as

$$\delta_\rho \equiv \arg\left[\frac{A_S(K_1 \to K\rho) \times A_P(\rho \to \pi\pi)}{A_S(K_1 \to K^*\pi) \times A_P(K^* \to K\pi)}\right]. \quad (53)$$

Note that the total relative phase, which is contained in the $\mathcal{J}$-function, contains of course the complex phase of the denominator of Breit-Wigner of the isobar. For the conventions necessary to define δ_ρ, we refer to Appendix B.

δ_ρ is independent of the conventional phase factors of the meson states (e.g. meson wave functions[12]). In the $^3P_0$ model, each decay amplitude is real, with suitable conventions of the wave functions and by factorization of spherical harmonics. Then in the quark model, δ_ρ is real. This is due to specific properties of the transition operator.

1. Sign of D/S Ratio

The simplest prediction is the one concerning the D/S ratio in the $b_1 \to \omega\pi$ and $a_1 \to \rho\pi$ decays. Indeed, this sign depends only on the well-known standard conventions. It is then striking that all the signs are correctly predicted by the model. In the case of b_1 and a_1, these signs are well measured and given in PDG. For the $K_1 \to K^*\pi$ channel, the signs are not given by Daum *et al.* in Ref. [8]. However, we can read the relative phase for $K_1(1270)$ from Fig. (13) in Ref. [8], which is positive ($f_{b5}/f_{b1} > 0$), while for $K_1(1400)$ we have to rely on the analysis of *BABAR* because it is not possible to fix it from the figure, since the D-wave is too weak and is overwhelmed compared to the D-wave of $K_1(1270)$ ($f_{a5}/f_{a1} < 0$).

In the paper of Gronau *et al.* [1,2], the D/S phase for $K^*\pi$ is given as $\delta_{D/S} = (260 \pm 20)°$. We believe that the authors were misled by incorrect interpretation of Fig. (13) (bottom-right) in Ref. [8]: The plotted phase indeed peaks at 260° at $M_{K\pi\pi} \approx 1.4$ GeV/c^2. But this is not the phase we are looking for, since it contains the phase from the Breit-Wigner of $K_1(1270)$, which is dominating the $K_1(1400)$ contribution and gives an additional phase of approximately 90°. Hence, the phase we are interested in must be read as $\delta_{D/S} \approx (260 - 90)° \sim 180°$. We must stress the following subtle point: The plotted phase is the difference of the phases of the D-wave strongly dominated by $K_1(1270)$ and the one of the S-wave, which includes large contributions of both resonances. As a consequence, paradoxically there appears a bump in the D-wave phase diagram, peaked at $M_{K\pi\pi} \sim (1.3\text{–}1.4)$ GeV/c^2, which is essentially determined by the tail of the Breit-Wigner of $K_1(1270)$. We checked this conclusion by explicit

[12] In the QPCM, δ_ρ can be calculated from

$$\delta_\rho \propto \arg\left[\frac{\psi^{(K_1)}\psi^{(K)*}\psi^{(\rho)*} \times \psi^{(\rho)}\psi^{(\pi)*}\psi^{(\pi)*}}{\psi^{(K_1)}\psi^{(K^*)*}\psi^{(\pi)*} \times \psi^{(K^*)}\psi^{(K)*}\psi^{(\pi)*}}\right] = \arg\left[\frac{\psi^{(K_1)}\psi^{(K)*}\psi^{(\pi)*}\psi^{(\pi)*}}{\psi^{(K_1)}\psi^{(K)*}\psi^{(\pi)*}\psi^{(\pi)*}}\right] = 1, \quad (54)$$

which implies that the relative phase of the total amplitudes is real (i.e. $\delta_\rho = 0$ or π) and does not depend on the separate complex phases of the meson wave functions.

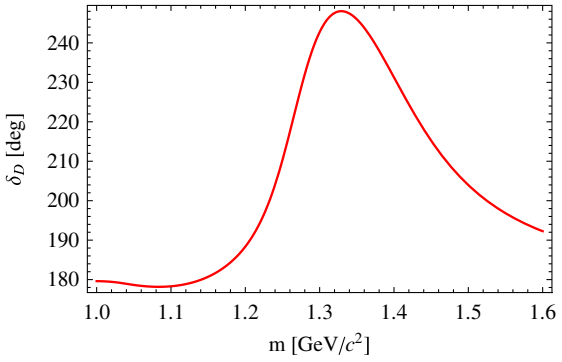

FIG. 6 (color online). The D-wave phase relative to the S-wave of $K^*\pi$, calculated using the K-matrix couplings. One can see a bump at $M_{K\pi\pi} \sim (1.3\text{–}1.4)$ GeV/c^2.

calculation of the amplitudes using the K-matrix couplings (see Fig. 6).

2. Relative Sign of $K\rho/K^*\pi$ Couplings

We study the real phase (i.e. the relative sign) of the $K_1(1270) \to K^*\pi$ and $K_1(1270) \to K\rho$ amplitudes, which plays an important role in the λ_γ determination using the ω-method (due to the strong dependence on the phase of the interference term $\mathrm{Im}[\vec{n} \cdot (\vec{\mathcal{J}} \times \vec{\mathcal{J}}^*)]$). Indeed, the odd moments of ω change their sign if one changes the relative sign between the $K_1^+ \to K^+\rho^0 \to K^+\pi^-\pi^+$ and $K_1^+ \to K^{0*}\pi^+ \to K^+\pi^-\pi^+$ amplitudes. One has to notice that, in this case, this phase hardly can be extracted from the K-matrix analysis by Daum *et al.* [8] due to some unknown conventions (in particular, the order of particles that is significant for the determination of the couplings signs). We then rely on the recent analysis by the Belle Collaboration [15] of the $B \to J/\psi(\psi')K\pi\pi$ decay which gives more explicit explanation of the conventions.

Here we summarize what is new in the Belle $B \to J/\psi(\psi')K\pi\pi$ paper [15]. First we will list the general conclusions of this paper and then we will discuss some details of the Dalitz plot shown in this paper, which provides important information relating to our work.

3. General Conclusions of Study of $B \to J/\psi K\pi\pi$ by Belle Collaboration

This paper, in principle, focuses on the measurement of the branching ratios of $B^+ \to J/\psi K^+\pi^+\pi^-$ and $B^+ \to \psi' K^+\pi^+\pi^-$. Since the $K\pi\pi$ final state comes from various resonances (K_{res}), this analysis provides information on the $K_{\mathrm{res}} \to K\pi\pi$ strong decays. Since the $K_{\mathrm{res}} = K_1(1270)$ turned out to be a prominent component (for both J/ψ and ψ'), some detailed study of $K_1(1270) \to K\pi\pi$ has been done:

(i) The Dalitz plot for the three-body decays is shown. We discuss more details on this later.

TABLE VI. The fitted branching ratios of the K_1-decays measured by the Belle Collaboration in the analysis of $B \to J/\psi K\pi\pi$ decay [15].

Decay mode	PDG (%)	Fit 1 (%)	Fit 2 (%)
$K\rho$	42 ± 6	57.3 ± 3.5	58.4 ± 4.3
$K^*\pi$	16 ± 5	26.0 ± 2.1	17.1 ± 2.3
$K_0^*(1430)\pi$	28 ± 4	1.90 ± 0.66	2.01 ± 0.64

(ii) The intermediated two-body decay branching ratios have been redetermined (see Table VI). The branching ratios for the dominant decay modes, $K_1(1270) \to K\rho$ and $K_1(1270) \to K^*\pi$, are found to be slightly different from the previous measurements (PDG), although they are still in accordance with several standard deviations. On the other hand, the $K_1(1270) \to K_0^*(1430)\pi$ channel, which was supposed to have a large branching fraction ($\mathcal{B}(K_1(1270) \to K_0^*(1430)\pi) = (28 \pm 4)\%$) according to the previous measurements [8,39], was found to have a significantly smaller contribution on the order of 2% (see Table VI).

(iii) In addition, by floating the mass and width of the $K_1(1270)$ in an additional fit of the $B^+ \to J/\psi K^+\pi^+\pi^-$ data, a smaller mass of $(1248.1 \pm 3.3(\mathrm{stat}) \pm 1.4(\mathrm{syst}))$ MeV/c^2 and larger width $(119.5 \pm 5.2(\mathrm{stat}) \pm 6.7(\mathrm{syst}))$ MeV/c^2 were measured for the $K_1(1270)$. Of course, there is a correlation between the fact that the scalar $+ \pi$ component becomes much smaller and the fact that the $K^*\pi$ and $K\rho$ contributions become larger (see Table VI).

Here we want to draw attention of the reader to the conceptual difficulties raised by the definition of the $K_1(1270)$-width. In Fit 1, the K_1 width is the one given by PDG, while in Fit 2, the width was treated as a free parameter. Because of the threshold effect, one should not expect that the width measured by the Belle Collaboration [15] from the Breit-Wigner denominator at the peak should coincide with the one defined by PDG, although it should be much larger. One observes that the floated width is larger than the PDG value but it is still much smaller than 200 MeV/c^2, as we would expect from the calculation using the K-matrix formalism (see Table III).

One has to point out that the D-waves are not taken into account in the master formula of Belle. On the other hand, we found from the theoretical study that the D-wave of $K^*\pi$ can have a small but non-negligible effect. In principle, there are two bumps due to the presence of the D-wave, but it is found that the one located in the intersection region of the $M_{K\pi} \sim M_{K^*}$ and $M_{\pi\pi} \sim M_\rho$ on the Dalitz plot is masked by the dominating peak of ρ. Using a Monte Carlo simulation, we observed a second small but non-negligible bump at low $M_{\pi\pi}$ (see Fig. 7, in the center).

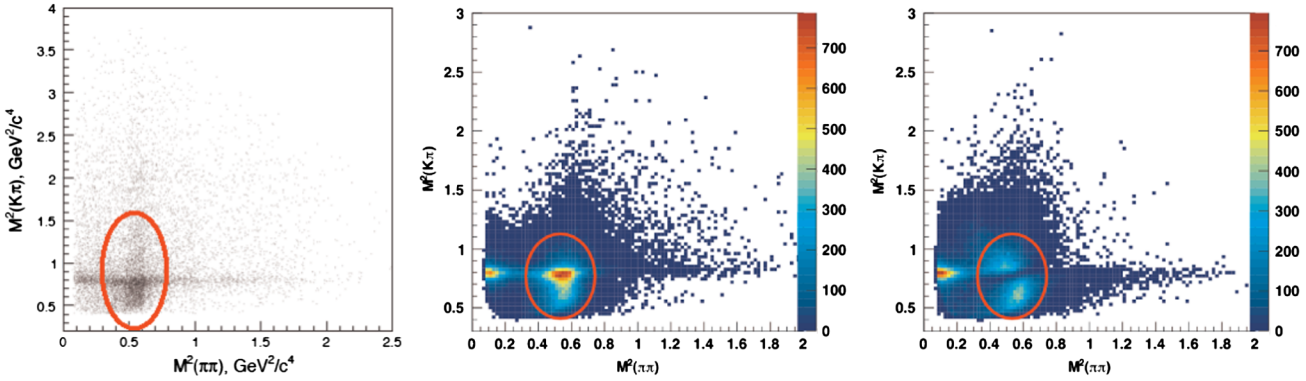

FIG. 7 (color online). Dalitz plots of $B^+ \to K_1^+(1270)\gamma \to K^+\pi^-\pi^+\gamma$, measured by the Belle Collaboration [15] (left) and Monte Carlo (MC) simulated for the offset phase equal to 0 (center) and π (right) of the $K\rho$ channel relative to $(K^*\pi)_S$. The "correct" phase $\delta_\rho = 0$ corresponds to our quark model prediction.

4. Dalitz Analysis

In Ref. [15], the Dalitz plots for $K_1(1270) \to K\pi\pi$ are shown in the three variable planes, $M^2(K^+\pi^+\pi^-)$, $M^2(K^+\pi^-)$, and $M^2(\pi^+\pi^-)$. On the Dalitz plot in the $M^2(K\pi) - M^2(\pi\pi)$ plane, a strong interference effect between $K_1 \to K^*\pi$ and $K_1(1270) \to K\rho$ is observed (see Fig. 7). In particular, it is pointed out that the weakening of the $K\rho$ in the region of $M(K\pi) > M_{K^*(892)}$ originates from the interference of the $K\rho$ and $K^*\pi$ amplitudes. Here we will attempt to study the real phase (in other words, the relative sign) of the $K_1 \to K^*\pi$ and $K_1(1270) \to K\rho$ amplitudes using this Dalitz plot to check our theoretical prediction. Indeed, as we will see in a forthcoming paper, this information of the phase has an important consequence on our λ_γ determination.

5. Determining Relative Sign of $K\rho/K^*\pi$ Amplitudes

In this section, we demonstrate how the relative phase between the $K\rho/K^*\pi$ amplitudes can be determined from the Dalitz plot.

In Ref. [15], the full amplitude of K_1 three-body decays is defined as

$$|\mathcal{M}(s_{K_1}, s_{K^*}, s_\rho)|^2 = |a_{K^*}A_{K^*}(s_{K_1}, s_{K^*}) + a_\rho A_\rho(s_{K_1}, s_\rho)|^2, \tag{55}$$

where the coefficients $a_{K^*,\rho}$ represent the strong decay of $K_1 \to K\pi\pi$ through K^*, ρ intermediate states. The amplitudes $A_{K^*,\rho}$ are defined as

$$A_V(s_{K_1}, s_V) = \frac{\sqrt{M_{K_1}\Gamma_{K_1}}}{M_{K_1}^2 - s - iM_{K_1}\Gamma_{K_1}} \times \frac{\sqrt{M_V\Gamma_V}}{M_V^2 - s_V - iM_V\Gamma_V} \times \sqrt{1 + \frac{\vec{p}_i^{\,2}}{s_{K_1}}\cos^2\theta_{ik}}, \tag{56}$$

where p_i is the breakup momentum of P_i or V in the K_1 reference frame and θ_{ik} is the angle between the momenta of P_i and P_k in the V reference frame, which can be expressed in terms of s_{K_1}, s_{ij}, s_{ik}.[13]

Compared to the obtained Dalitz plot, we can determine the coefficients $a_{K^*,\rho}$ including the relative phase between them. The obtained result by the Belle Collaboration [15] yields:

$$\begin{aligned} |a_{K^*}| &= 0.962 \pm 0.058 \pm 0.176, \\ |a_\rho| &= 1.813 \pm 0.090 \pm 0.243 \\ \delta_\rho &\equiv \arg(a_\rho/a_{K^*}) = -(43.8 \pm 4.0 \pm 7.3)^\circ \end{aligned} \tag{57}$$

Eq. (55) can be written in the following general form, factorizing out the phase:

$$\begin{aligned} |\mathcal{M}(s_{K_1}, s_{K^*}, s_\rho)|^2 = {} & c_0(s_{K_1}, s_{K^*}, s_\rho) \\ & + c_1(s_{K_1}, s_{K^*}, s_\rho)\cos\delta_\rho \\ & + c_2(s_{K_1}, s_{K^*}, s_\rho)\sin\delta_\rho, \end{aligned} \tag{58}$$

where $c_i(s, s_{K\pi}, s_{\pi\pi})$ are the known functions, expressed in terms of various combinations of the real and imaginary parts of $|a_{K^*}|A_{K^*}(s_{K_1}, s_{K^*})$ and $|a_\rho|A_\rho(s_{K_1}, s_\rho)$. So, to establish the correspondence between our parametrization of $|\mathcal{M}|^2$ ($|\vec{\mathcal{J}}|^2$ in our case, one can compare the relative signs of the $\cos\delta_\rho$ and $\sin\delta_\rho$ coefficients, $c_{1,2}$, on the Dalitz plot. Direct numerical calculation shows that

$$\begin{aligned} \text{sign}\,(c_1^{\text{model}}) &= \text{sign}(c_1^{\text{Belle}}), \\ \text{sign}(c_2^{\text{model}}) &= -\text{sign}(c_2^{\text{Belle}}). \end{aligned} \tag{59}$$

6. Issues of Complex Offset Phases

In principle, the QPCM predicts real $K_1 \to VP$ amplitudes without any complex phases. This should correspond to the K-matrix couplings. The complex rotation of the

[13] One has to notice that the D-wave amplitude is not taken into account in this parametrization and that the last factor in Eq. (56) corresponds to the S-wave.

K-matrix states to the physical states should introduce complex phases, but we found by explicit calculation that the imaginary part of the rotation angle is small:

$$\varphi_{a'\to a^{ph}} \simeq 10°. \tag{60}$$

However, the Belle Collaboration [15] measured a sizably larger imaginary relative phase [i.e. Eq. (57)] of $\delta_\rho \simeq -44°$. We recall also that Daum *et al.* [8] measured a nonzero phase of the order of 30°. Similar value was found in the reanalysis of the ACCMOR data by the *BABAR* Collaboration: $\delta_\rho = -31°$ [16].

There is no explanation of this complex phase in a definite theoretical model, neither in the $^3P_0$ quark model nor in the most general quasi-two-body K-matrix approach. Indeed, the offset phase which is introduced in the analysis by Daum *et al.* [8] depends only on the decay channel and is the same for the lower and upper resonances. The general production amplitude for each channel in the reaction $K^- p \to (K^-\pi^+\pi^-)$ is written as [8,16]

$$F_i = e^{i\delta_i}\sum_j (1 - iK\rho)^{-1}_{ij} P_j, \tag{61}$$

where the factor $(1 - iK)^{-1}$ represents the propagation and the decay of the K_1-resonance. The last factor, P_j, describes the resonance production which can be in principle complex (indeed, one finds in Ref. [8] that there is a nonzero relative phase between the production couplings of two K_1-resonances). From Eq. (61) it is obvious that the offset phase δ_i cannot be ascribed either to the resonance decay or the production amplitude.

This puzzling situation must not be ignored and has to be studied more carefully. In the present, we use the model prediction for the $\mathcal{J}$-function as it is with pure real couplings. On the other hand, to adopt a pragmatic attitude we explore the effect of introducing this additional offset phase $\delta_\rho = -\delta_\rho^{\text{Belle}}$ in the calculation of the $\mathcal{J}$-function and the estimation of the theoretical uncertainty of λ_γ.

D. Issue of $\kappa\pi$ Channel

The PDG assigns a large branching ratio $\mathcal{B}(K_1(1270) \to K_0^*(1430)\pi) = (28 \pm 4)\%$. It is extracted, as with all the branching ratios, from ACCMOR data and analysis. [8] However, this interpretation is dubious. The original ACCMOR measurement shows indeed a clear, strongly coupled peak in the scalar + π channel around the mass $M_{K\pi\pi} \sim 1270$ MeV/c^2. However, it is not at all claimed that the scalar is $K_0^*(1430)$; it is treated as a lower and much broader scalar meson ($M \simeq 1.25$ GeV/c^2, $\Gamma \simeq 600$ MeV/c^2); or it could be a continuum $(K\pi)_{S-\text{wave}}$, according to Ref. [40].

The $K_0^*(1430)$-meson is the scalar orbitally excited state of kaon, which has the mass $M_{K_0^*(1430)} = (1425 \pm 50)$ MeV/c^2 and width $\Gamma_{K_0^*(1430)} = (270 \pm 80)$ MeV/c^2 [39]. According to quark models, the constituent quarks are in the $^3P_0$ state. In order to estimate the $K_0^*(1430)\pi$ contribution, we use QPCM to calculate the P-wave amplitude for the decays $K_1(1270) \to K_0^*(1430)\pi$. One can see from Fig. 8 that $A_P(K_1(1270) \to K_0^*(1430)\pi)$ is strongly suppressed compared to $A_S(K_1(1270) \to K^*\pi)$. Moreover, there is also a suppression due to the phase space. Finally, after the integration over the phase space for $\sqrt{s_{K\pi}}$ within the allowed physical range $[m_K + m_\pi; M_{K_1(1270)} - m_\pi]$, we predict that

$$\frac{\mathcal{B}(K_1(1270) \to K_0^*(1430)\pi)}{\mathcal{B}(K_1(1270) \to K^*(892)\pi)} < 0.01\%, \tag{62}$$

in blatant contradiction to the PDG entry.

What is most striking is that, indeed, the Belle Collaboration [8] finds $\mathcal{B}(K_1(1270) \to K_0^*(1430)\pi) \simeq 2\%$ (see Table VI); it is very small, as we predict. They did not find any other lower scalar + π component in the K_1-decay: The $\mathcal{B}$ missing with respect to ACCMOR [8] seems to be filled by an enlargement of $K\rho$. Therefore, in our analysis, we do not include the $K_1(1270) \to K_0^*(1430)\pi$ channel. Neither do we include any other possible scalar in the presented results. However, to take into account the contrary conclusions of ACCMOR, we keep in mind the possibility that there is some significant portion of the branching ratio carried by a very wide scalar meson, different from the $K_0^*(1430)$, such as the low-lying state $K_0^*(800)$ (also called κ) [41]. Note that such a state is most probably not a $q\bar{q}$ state, and therefore the decay into $\kappa\pi$ cannot be estimated within our theoretical model. Such a contribution has not been tested explicitly in the analysis by the Belle Collaboration. [15]

Let us mention two other relevant facts. On one hand, the nonstrange counterpart of $\kappa(800)$, σ, is found with sizable branching ratio in the decay of $a_1(1260)$ in the $\sigma\pi$ state. On the other hand, it is surprising, as noticed by Daum *et al.* [8], that there is no $\kappa\pi$ channel in the $K_1(1400)$-decay.

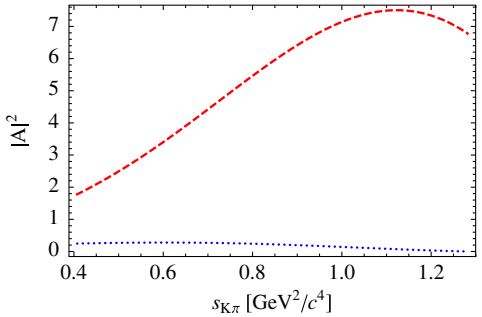

FIG. 8 (color online). $|A_S(K_1(1270) \to K^*\pi)|^2$ (dashed line) and $|A_P(K_1(1270) \to K_0^*(1430)\pi)|^2$ (dotted line) for $s_{K_1} = M^2_{K_1(1270)}$. The K_1 mixing angle θ_{K_1} is taken to be 60°.

VI. CONCLUSIONS

Let us now summarize the main conclusions of the present work, and sketch some prospects for progress regarding theory as well as experience.

Not only is the strong decay pattern of K_1-mesons quite complex, but not surprisingly, it is also difficult to analyze the whole system experimentally. In spite of many efforts, we have found that much information is lacking, and that certain weaknesses may be suspected in various analyses. For lack of more fundamental treatments, we have taken recourse in the quark model approach to explain and complement the experimental results. The quark model, although approximate, is the basis of our whole understanding of spectroscopy. The $^3P_0$ model for decays presents the advantage of handling in a simple way the whole set of $L = 1$ decays.[14] On the other hand, experimental input is still required to fix necessary parameters; for instance, the K_1 mixing angle.

Our predictions for the specific strong decays under concern, i.e. $L = 1$ states decaying to VP states, can be evaluated by comparing to data where available. On the whole, our conclusion is very encouraging. In addition to the known fact that a certain mixing is able to explain the pattern of VP decays, the model explains detailed features which are quite outside an $SU(3)$ symmetry approach and require a dynamical approach. This is the case, for instance, with the D/F ratio of octet couplings and the D/S ratios in magnitude and phase; it is an achievement of the model that all the observable phases are correctly predicted. Another typically dynamical prediction is that the decays to $q\bar{q}$ scalar + pseudoscalar should be very small. It is in agreement with the recent observations by Belle [15], but it does not exclude a large contribution of non $q\bar{q}$ scalars, which could then explain the observations of ACCMOR. [8] In any case, it strengthens the conclusion that the κ channel observed by ACCMOR is not the $K_0^*(1430)$ (presumed $q\bar{q}$), as tabulated in the PDG tables.

We believe that the K_1 system deserves further investigation because it has revealed various interesting aspects. Indeed, it also presents unexplained features in the standard domain of spectroscopy, i.e. the mixing angle and the mass splitting. The mixing of the two states offers the possibility to explain the remarkable pattern of $K^*\pi/K\rho$ decays, but the angle is not a theoretical prediction. In fact, in a potential model, spin-orbit forces generate a mixing, but it is not the one which is observed. As explained in the text, loop effects would also generate a mixing effect, but it cannot be calculated. It must also be noted that the mixing does not explain why the $\kappa\pi$ channel, if present in $K_1(1270)$, is absent in $K_1(1400)$: Quite the contrary, as explained in Daum *et al.* [8], one would expect the mixing to generate a coupling from the K_A component. Apart from mixing, the predictions of the potential model also fail to explain the splitting of the two states—it is predicted to be much too small by the model of Godfrey and Isgur [22], which can be estimated to be the most trustworthy. These facts show that our knowledge of spectroscopy is not yet satisfactory, even for apparently well identified, low-lying $q\bar{q}$ states. Understanding these facts, then, justifies further studies.

We try to say something about possible improvements:

(1) *Improvement of the Theoretical Treatment*. It is important to recall that there is no fundamental theoretical treatment of such problems and that quark models on which our theoretical model is based, although very valuable, contain essential approximations, i.e. ones that cannot be improved systematically. This holds in two respects: Potential models are of course essentially approximate, even with relativistic improvements such as that included in the model of Godfrey and Isgur [22], but this is also true of the quark-pair-creation decay model itself which, presently, is essentially nonrelativistic. The center of mass motion of the hadrons is not treated relativistically. Progress is desirable in this direction.

(2) *Prospects of Improvement of Experimental Knowledge*. At present, further progress could come mainly from a better and more complete determination of the magnitudes and the phases of the various couplings through experiments. Certainly, the old experiments with production of K_1 by strong interaction scattering, as the ones in SLAC [7] and ACCMOR, [8] have much larger statistics for decays involving K_1 than present B factories. Yet there is little prospect of them being redone, and they also have their own weakness in the fact that the production process is complex. On the other hand, there is the hope that new, detailed studies could be made in B- and τ-decays. Encouraging examples have been coming both from *BABAR* and Belle, such as $\tau \to K_1\nu_\tau$ [42] and $B \to K_1\psi$ [15]. In fact, a distribution in an additional angle may also help to improve the analysis. For example, a new study of $B \to K_1\psi$ with angular analysis could yield directly the crucial quantity $\mathrm{Im}(\vec{n}\cdot(\vec{\mathcal{J}}\times\vec{\mathcal{J}}^*))$ up to a multiplicative constant [3]. The analyses could be guided by our semitheoretical and approximate investigation, which, for instance, emphasizes the need to take into account D waves, not included in the present Belle analysis of $B \to K_1\psi$.

ACKNOWLEDGMENTS

We thank very much Damir Becirevic for his critical discussions and comments and for constant help. Alain Le Yaouanc acknowledges constant discussions with his coworkers Luis Oliver and Jean-Claude Raynal. A. T. thanks

[14] In fact, it is supported by a much larger set of experimental tests.

Olivier Pène for his precious help. We would like to thank W. Dunwoodie, S. Émery, Y. Sakai, K. Trabelsi, M. Nakao, and S. Hashimoto for very useful discussions and provided information. This work was supported in part by the ANR contract "LFV-CPV-LHC" ANR-NT09-508531 and the France-Japan corporation of IN2P3/CNRS TYL-LIA.

APPENDIX A: REINTERPRETING ACCMOR RESULT IN TERMS OF PHYSICAL STATES

In order to determine our model parameters and the K_1 mixing angle from comparison of the predicted partial decay widths of the K_1-meson decays into the dominant $K^*\pi$ and $K\rho$ channels with the measured experimental values, we use the fitted K-matrix parameters extracted by Daum *et al.* from Ref. [8].

Using the definition of the K_1 mixing by Daum *et al.*, [8] (which is different from Eq. (2) that we use by signs):

$$\begin{aligned}|K_1(1400)\rangle &= |K_{1A}\rangle\cos\theta_{K_1} + |K_{1B}\rangle\sin\theta_{K_1}|K_1(1270)\rangle \\ &= -|K_{1A}\rangle\sin\theta_{K_1} + |K_{1B}\rangle\cos\theta_{K_1}.\end{aligned} \tag{A1}$$

The dominant S-wave K-matrix couplings of the K_1s to the states $K^*\pi$ (Channel 1) and $K\rho$ (Channel 2) are given as [8]

$$\begin{aligned}f_{a'1} &= \frac{1}{2}\gamma_+\cos\theta_{K_1} + \sqrt{\frac{9}{20}}\gamma_-\sin\theta_{K_1} \\ f_{b'1} &= -\frac{1}{2}\gamma_+\sin\theta_{K_1} + \sqrt{\frac{9}{20}}\gamma_-\cos\theta_{K_1} \\ f_{a'2} &= \frac{1}{2}\gamma_+\cos\theta_{K_1} - \sqrt{\frac{9}{20}}\gamma_-\sin\theta_{K_1} \\ f_{b'2} &= -\frac{1}{2}\gamma_+\sin\theta_{K_1} - \sqrt{\frac{9}{20}}\gamma_-\cos\theta_{K_1},\end{aligned} \tag{A2}$$

where γ_+ and γ_- are the reduced $SU(3)$ couplings for K_{1A} (F-type) and K_{1B} (D-type), respectively. Their fitted experimental values are given in Table VII. The indices a' and b' denote the upper and lower K_1 resonances, respectively.

Using the experimental values of the K-matrix couplings from Table VIII and performing the diagonalization of the complex mass matrix [Eq. (31)], we observed that

TABLE VII. Fitted K-matrix pole masses, S-wave reduced $SU(3)$ couplings, and mixing angle for K_{1A} (F-type) and K_{1B} (D-type), taken from Ref. [8] (low t data). The indices a' and b' denote the upper and lower K_1 resonances, respectively.

$m_{a'}$, GeV/c^2	$m_{b'}$, GeV/c^2	γ_+	γ_-	$\tilde{\theta}_{K_1}$
1.4 ± 0.02	1.17 ± 0.02	0.78 ± 0.1	0.54 ± 0.1	$64° \pm 8°$

(i) The variation of the absolute values and phases of the new rotated physical couplings $\{f_{a^{ph}i}, f_{b^{ph}i}\}$ around the masses at the peak of Breit-Wigner (i.e. $m \sim 1.27$ GeV/c^2 and 1.4 GeV/c^2) turn out to be small (see Fig. 9).

(ii) Contribution of the complex phase space for energy below the decay threshold (which implies $\rho_{ij}(m) \to i|\rho_{ij}(m)|$) is very small for diagonalized physical mass of $K_1(1400)$ (see Fig. 10). But one observes a threshold effect for $K_1(1270)$ near $m \sim 1.2$ GeV/c^2. However, the mass variation of $M_{K_1}(m)$ around the peak of Breit-Wigner can be considered not so significant.

(iii) One can see from Fig. 10 that, contrary to $M_{K_1}(m)$ dependence, the width $\Gamma_{K_1}(m)$ is a rapidly varying function of the energy m.

(iv) Nondiagonal elements of the mass matrix (31) are sufficiently small compared to the diagonal ones. One can see from Fig. 10 that the difference between the properly diagonalized masses and widths (blue/red curves), which are calculated in terms of the rotated physical couplings, and the real and imaginary parts of the diagonal elements of (31) (green/orange curves) is insignificant. As a consequence, our assumption for the partial widths

$$\Gamma_{a^{ph}i}(M_{\text{peak}}) \simeq \Gamma_{a'i}(M_{\text{peak}}) = \Gamma^{\text{QPCM}}_{a'i}(M_{\text{peak}}) \tag{A3}$$

seems to be reasonable. This means that we can use the experimental measured K-matrix couplings to calculate the partial decay widths and fit our model parameters, namely, quark-pair-creation constant γ and the mixing angle θ_{K_1}, which can further be used for the $\mathcal{J}$ function computation.

TABLE VIII. K-matrix couplings, calculated from Eq. (A2) using the fitted parameters from Table VII. The indices a' and b' denote the upper and lower K_1 resonances, respectively, decaying into $K^*\pi$ (channel 1) and $K\rho$ (channel 2) hadronic states, respectively. The coupling to the $K_0^*(1430)\pi$ channel, where $K_0^*(1430)$ resonance is supposed to have the mass 1.25 GeV/c^2 and width 600 MeV/c^2, f_{b3} is taken from Ref. [16].

$f_{a'1}$	$f_{b'1}$	$f_{a'2}$	$f_{b'2}$	$f_{a'3}$	$f_{b'3}$
0.50 ± 0.07	-0.19 ± 0.09	-0.15 ± 0.10	-0.51 ± 0.06	0	0.32

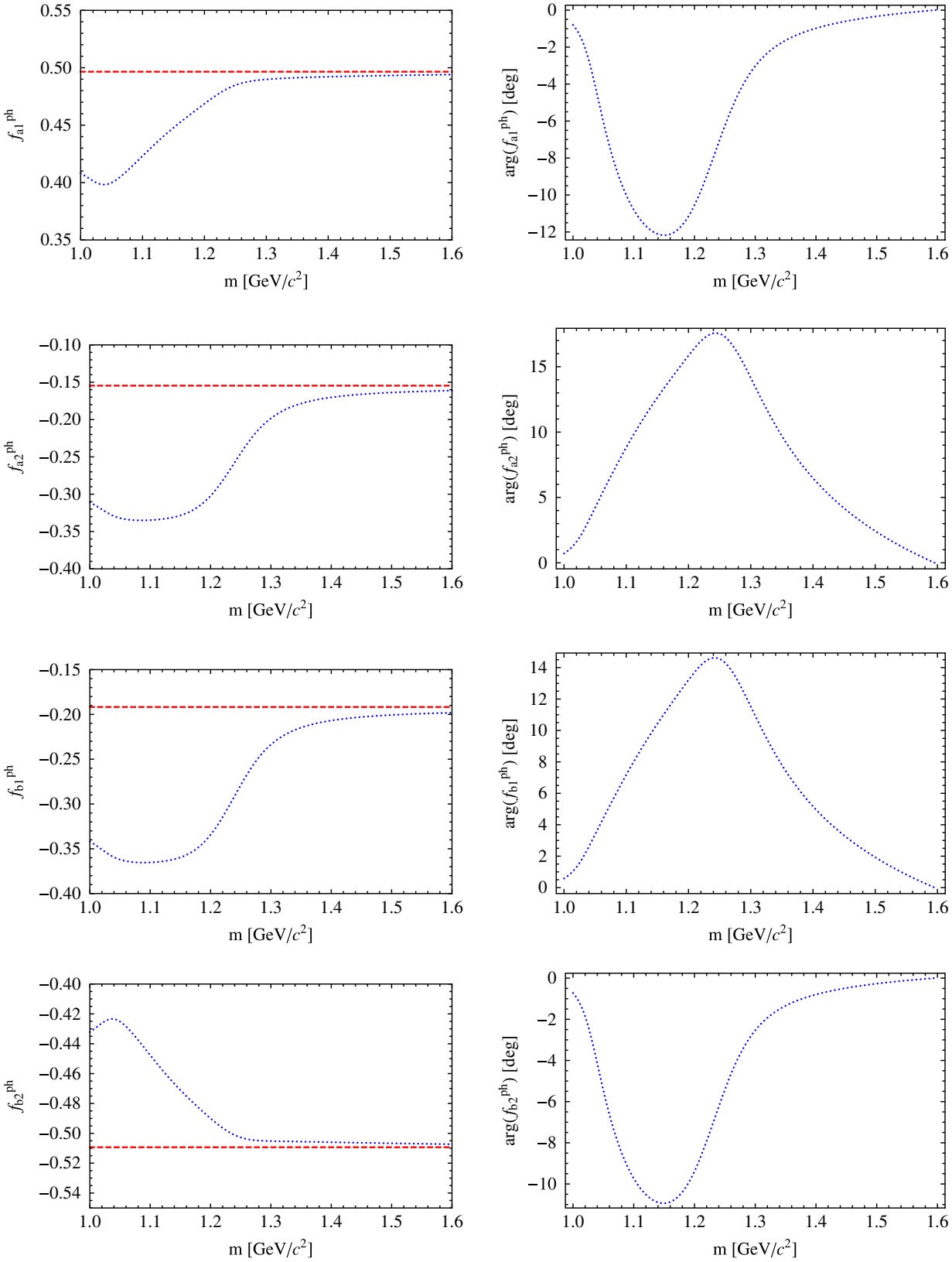

FIG. 9 (color online). Energy dependence of the physical couplings (dotted lines). The dashed lines represent the values of the real couplings for the K-matrix states, fitted by the ACCMOR Collaboration [8].

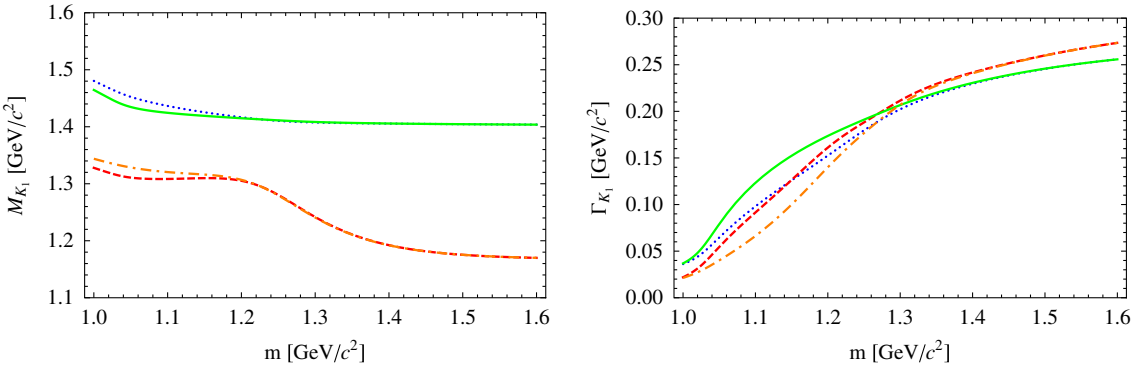

FIG. 10 (color online). Energy dependence of the mass (left) and width (right) of $K_1(1270)$ (dashed, dash-dotted lines) and $K_1(1400)$ (dotted, solid lines). Dashed and dotted curves correspond to the masses and total widths of the physical eigenstates, i.e. diagonal mass matrix elements which are calculated in terms of the rotated physical couplings. Dash-dotted and solid curves represent the leading diagonal elements of the complex mass matrix $(M' - i\Gamma'/2)_{a'b'}$ in the K-matrix eigenstate basis. The D-wave contribution is not taken into account due to the absence of knowledge of the corresponding couplings.

APPENDIX B: QPCM

1. Spatial Integrals in QPCM

For the decay $A \to B + C$ (see Fig. 1), the spacial integrals are given by

$$\begin{aligned} I_m^{(ABC)} &= \int d^3\vec{k}_1 d^3\vec{k}_2 d^3\vec{k}_3 d^3\vec{k}_4 \delta(\vec{k}_1 + \vec{k}_2 - \vec{k}_A) \\ &\quad \times \delta(\vec{k}_2 + \vec{k}_3 - \vec{k}_B)\delta(\vec{k}_4 + \vec{k}_1 - \vec{k}_C)\delta(\vec{k}_3 + \vec{k}_4) \\ &\quad \times \mathcal{Y}_1^m(\vec{k}_3 - \vec{k}_4)\psi^{(A)}(\vec{k}_1 - \vec{k}_2)\psi^{(B)}(\vec{k}_2 - \vec{k}_3) \\ &\quad \times \psi^{(C)}(\vec{k}_4 - \vec{k}_1) \\ &= \frac{1}{8}\int d^3\vec{k}\,\mathcal{Y}_1^m(\vec{k}_B - \vec{k})\psi^{(A)}(\vec{k}_B + \vec{k}) \\ &\quad \times \psi^{(B)}(-\vec{k})\psi^{(C)}(\vec{k}), \end{aligned} \tag{B1}$$

where ψs are the normalized Fourier transforms of harmonic oscillator meson wave functions. The wave functions for the ground ($L = 0$) and orbitally excited ($L = 1$) meson states are defined as

$$\psi_0^{(i)}(\vec{k}) = \frac{R_i^{3/2}}{\pi^{3/4}}\exp\left(-\frac{\vec{k}^2R_i^2}{8}\right) \qquad (L=0)$$

$$\psi_1^{m(i)}(\vec{k}) = \sqrt{\frac{2}{3}}\frac{R_i^{5/2}}{\pi^{1/4}}\mathcal{Y}_1^m(\vec{k})\exp\left(-\frac{\vec{k}^2R_i^2}{8}\right)$$

$$(L=1, L_z=m) \qquad \mathcal{Y}_1^m(\vec{k}) = |\vec{k}|Y_1^m(\hat{\vec{k}}) = (\vec{\varepsilon}_m\vec{k})\sqrt{\frac{3}{4\pi}}. \tag{B2}$$

Here, R_i is the meson wave function radius and $\vec{\varepsilon}_m$ are the A-polarization vectors, defined as

$$\vec{\varepsilon}_0 = \begin{pmatrix} 0 \\ 0 \\ 1 \end{pmatrix}, \qquad \vec{\varepsilon}_{\pm 1} = \mp\frac{1}{\sqrt{2}}\begin{pmatrix} 1 \\ \mp i \\ 0 \end{pmatrix}. \tag{B3}$$

Performing the integration over $\vec{k}$, one obtains for the orbitally excited axial-vector meson decay into pseudoscalar and vector mesons in the A-meson reference frame:

$$\begin{aligned} I_m^{(ABC)} &= -\frac{4\sqrt{3}}{\pi^{5/4}}\frac{R_A^{5/2}(R_BR_C)^{3/2}}{(R_A^2+R_B^2+R_C^2)^{5/2}}\Bigg((\vec{\varepsilon}_m\cdot\vec{\varepsilon}_{-m}) \\ &\quad -(\vec{\varepsilon}_m\cdot\vec{k}_B)(\vec{\varepsilon}_{-m}\cdot\vec{k}_B)\frac{(2R_A^2+R_B^2+R_C^2)(R_B^2+R_C^2)}{4(R_A^2+R_B^2+R_C^2)}\Bigg) \\ &\quad \times\exp\left[-\vec{k}_B^2\frac{R_A^2(R_B^2+R_C^2)}{8(R_A^2+R_B^2+R_C^2)}\right]. \end{aligned} \tag{B4}$$

Setting $\vec{k}_B$ along z-axis, the integrals become

$$\begin{aligned} I_0^{(ABC)} &= -\frac{4\sqrt{3}}{\pi^{5/4}}\frac{R_A^{5/2}(R_BR_C)^{3/2}}{(R_A^2+R_B^2+R_C^2)^{5/2}} \\ &\quad \times\left(1-\vec{k}_B^2\frac{(2R_A^2+R_B^2+R_C^2)(R_B^2+R_C^2)}{4(R_A^2+R_B^2+R_C^2)}\right) \\ &\quad \times\exp\left[-\vec{k}_B^2\frac{R_A^2(R_B^2+R_C^2)}{8(R_A^2+R_B^2+R_C^2)}\right] \\ I_1^{(ABC)} &= \frac{4\sqrt{3}}{\pi^{5/4}}\frac{R_A^{5/2}(R_BR_C)^{3/2}}{(R_A^2+R_B^2+R_C^2)^{5/2}} \\ &\quad \times\exp\left[-\vec{k}_B^2\frac{R_A^2(R_B^2+R_C^2)}{8(R_A^2+R_B^2+R_C^2)}\right]. \end{aligned} \tag{B5}$$

For the vector meson ground state decay into two pseudoscalar mesons, the spacial integral is

$$\begin{aligned} I_m^{(ABC)} &= \frac{\sqrt{6}}{\pi^{5/4}}(\vec{\varepsilon}_m\cdot\vec{k}_C)\frac{(R_AR_BR_C)^{3/2}(2R_A^2+R_B^2+R_C^2)}{(R_A^2+R_B^2+R_C^2)^{5/2}} \\ &\quad \times\exp\left[-\vec{k}_C^2\frac{R_A^2(R_B^2+R_C^2)}{8(R_A^2+R_B^2+R_C^2)}\right]. \end{aligned} \tag{B6}$$

B. Fixing Relative Signs for Three-Body Decay

Clebsch-Gordan Coefficients

As it was emphasized in the main text, the relative sign of several amplitudes involving various intermediate states plays a very important role. Therefore, the convention of the particle order in the Clebsch-Gordan coefficients is very important. For instance, for the case of $K_1^+ \to K^+\pi^-\pi^+$ decay, that implies that we take the Clebsch-Gordan coefficients defined in the following way:

$$\begin{aligned}(K^{*0}\pi^+|K_1^+) &= (1/2,-1/2;1,1|1/2,1/2) = -\sqrt{\frac{2}{3}}\\ (K^+\pi^-|K^{*0}) &= (1/2,1/2;-1,1|-1/2,1/2) = +\sqrt{\frac{2}{3}}\\ (K^+\rho^0|K_1^+) &= (1/2,1/2;1,0|1/2,1/2) = +\frac{1}{\sqrt{3}}\\ (\pi^-\pi^+|\rho^0) &= (1,-1;1,1|1,0) = -\frac{1}{\sqrt{2}}.\end{aligned} \tag{B7}$$

This gives the signs of the amplitudes listed in Table II.

3. Determination of Relative Sign of $g_{K^*K\pi}$ and $g_{\rho\pi\pi}$

Following the definition in the work of Gronau *et al.*, the total amplitude of the two possible channels is written as

$$\begin{aligned}\mathcal{M}^{(a)} &= \varepsilon_\mu^{(K_1)} T^{\mu\nu}_{K^*\pi} \varepsilon_\nu^{(K^*)*} g_{K^*K\pi} \varepsilon_\sigma^{(K^*)} (p_{\pi^-} - p_{K^+})^\sigma\\ \mathcal{M}^{(b)} &= \varepsilon_\mu^{(K_1)} T^{\mu\nu}_{K\rho} \varepsilon_\nu^{(\rho)*} g_{\rho\pi\pi} \varepsilon_\sigma^{(\rho)} (p_{\pi^+} - p_{\pi^-})^\sigma,\end{aligned} \tag{B8}$$

where $T^{\mu\nu}_{VP}$ is the hadronic tensor, parametrized in terms of the form factors f_V, h_V (or equivalently the S and D partial wave amplitudes).[15]

Now, using the same Clebsch-Gordan coefficients, defined previously in Eq. (B7), one can write the amplitude of the $V \to PP$ decay, calculating the general tensor Lorenz-invariant form in the vector meson reference frame:

$$\begin{aligned}\mathcal{M}(K^{*0} \to K^+\pi^-) &= -\sqrt{\frac{2}{3}} g_{K^*K\pi} (\vec{\varepsilon}_{K^*} \cdot (\vec{p}_{\pi^-} - \vec{p}_{K^+}))\\ &= \sqrt{\frac{8}{3}} g_{K^*K\pi} (\vec{\varepsilon}_{K^*} \cdot \vec{p}_{K^+})\\ \mathcal{M}(\rho^0 \to \pi^-\pi^+) &= \sqrt{\frac{1}{2}} g_{\rho\pi\pi} (\vec{\varepsilon}_\rho \cdot (\vec{p}_{\pi^+} - \vec{p}_{\pi^-}))\\ &= -\sqrt{2} g_{\rho\pi\pi} (\vec{\varepsilon}_\rho \cdot \vec{p}_{\pi^-}).\end{aligned} \tag{B9}$$

Taking into account all the spin and isospin couplings, the QPCM prediction is

$$\begin{aligned}\mathcal{M}_m^{\mathrm{QPCM}}(K^{*0} \to K^+\pi^-) &= -\frac{1}{6}\gamma I_m^{(K^*K\pi)}\\ &= -\frac{1}{6}\gamma \tilde{I}^{(K^*K\pi)} (\vec{\varepsilon}_m \cdot \vec{p}_{K^+})\\ \mathcal{M}_m^{\mathrm{QPCM}}(\rho^0 \to \pi^-\pi^+) &= -\frac{1}{3\sqrt{2}}\gamma I_m^{(\rho\pi\pi)}\\ &= -\frac{1}{3\sqrt{2}}\gamma \tilde{I}^{(\rho\pi\pi)} (\vec{\varepsilon}_m \cdot \vec{p}_{\pi^-}),\end{aligned} \tag{B10}$$

where $\tilde{I}^{(VPP)}$ can be defined from Eq. (B6).[16]

Now, doing a match between two approaches and factorizing out the common factor $\vec{\varepsilon} \cdot \vec{p}_i$, we can write the following equations:

$$\sqrt{\frac{8}{3}} g_{K^*K\pi} = -\frac{1}{6}\gamma \tilde{I}^{(K^*K\pi)} - \sqrt{2} g_{\rho\pi\pi} = -\frac{1}{3\sqrt{2}}\gamma \tilde{I}^{(\rho\pi\pi)}. \tag{B11}$$

Since $\tilde{I}^{(VPP)}$ is a positive function, one can see that

$$\mathrm{sign}\,(g_{K^*K\pi}) = -\mathrm{sign}(g_{\rho\pi\pi})$$

and in the $SU(3)$ limit $\frac{g_{\rho\pi\pi}}{g_{K^*K\pi}} = -\sqrt{\frac{8}{3}}$.

One can notice that the choice of the order in the isospin factors of the vector meson decay into two pseudoscalars in Eq. (B7) well fixes the relative sign of the g_{VPP} couplings. Moreover, this method makes the calculation of the quasi-two-body decay amplitude independent of the intermediate vector meson state (K^*, ρ) wave function sign (which, in principle, can be arbitrary in the quasi-two-body calculation since the final state is not the same).

APPENDIX C: PARTIAL WAVE AMPLITUDES

With the quark models, one can directly calculate the amplitudes with definite spin or helicity states. An experiment can measure the partial wave amplitudes of particular quantum numbers of the final state. Since both canonical (orbital) and helicity approaches give complete description of the process, one can find the relation between two representations for the decay of the initial at-rest state $|J, M\rangle$ with spin J and spin projection M onto the z-axis into two particles with spins $s_{1,2}$, helicities $\lambda_{1,2}$, total spin S, and relative orbital momentum L [43]:

$$\mathcal{M}^{JM}_{\lambda_1\lambda_2}(\Omega_1) = N_J f^J_{\lambda_1\lambda_2} D^{J*}_{M,\lambda_1-\lambda_2}(\Omega_1) \tag{C1}$$

with the normalization factor $N_J = \sqrt{\frac{2J+1}{4\pi}}$.

[15]For a more detailed definition of the hadronic tensor $T^{\mu\nu}$ and its parametrization in terms of two form factors, f_V and h_V, see Ref. [3].

[16]One has to be careful with the choice of the momentum, i.e. $\vec{p}_C$ or $\vec{p}_B = -\vec{p}_C$, since it changes the sign of the P-wave amplitude.

The observed number of events is given by

$$\sum_{M,\lambda_i,\lambda_i'} \int \mathcal{M}^{JM}_{\lambda_1\lambda_2}(\Omega_1)\mathcal{M}^{JM*}_{\lambda_1'\lambda_2'}(\Omega_1)d\Omega_1 = 4\pi \sum_{\lambda_i,\lambda_i'\lambda_1-\lambda_2=\lambda_1'-\lambda_2'} N_J^2 f^J_{\lambda_1\lambda_2} f^{J*}_{\lambda_1'\lambda_2'}. \quad \text{(C2)}$$

The recoupling from the canonical to the helicity representation is

$$N_J f^J_{\lambda_1\lambda_2} = \sum_{L,S} \sqrt{2L+1}(L,0;S,\lambda_1-\lambda_2|J,\lambda_1-\lambda_2) \times (s_1,\lambda_1;s_2,-\lambda_2|S,\lambda_1-\lambda_2)A_L. \quad \text{(C3)}$$

The two-body decay of the axial-vector meson into vector and pseudoscalar mesons can proceed in S- and D-waves. Using $J=1$, $\lambda_1=\lambda_V$, $\lambda_2=0$, the helicity amplitudes in the A reference frame can be written in terms of partial wave amplitudes:

$$N_1 f^1_{\lambda_V 0} = \sum_{L=0,2} \sqrt{2L+1}(L,0;1,\lambda_V|1,\lambda_V)A_L. \quad \text{(C4)}$$

Setting $\vec{k}_V$ along z-direction (i.e. $\theta_V=0$), the helicity amplitudes are

$$\mathcal{M}^{10}_{00} = N_1 f^1_{00} = A_S - \sqrt{2}A_D$$
$$\mathcal{M}^{1,\pm1}_{\pm1,0} = N_1 f^1_{\pm1,0} = A_S + \frac{1}{\sqrt{2}}A_D. \quad \text{(C5)}$$

By turns, the partial wave amplitudes are related to the helicity amplitudes as follows:

$$A_S = \frac{1}{3}(2\mathcal{M}^{11}_{10} + \mathcal{M}^{10}_{00}) \qquad A_D = \frac{\sqrt{2}}{3}(\mathcal{M}^{11}_{10} - \mathcal{M}^{10}_{00}). \quad \text{(C6)}$$

Summing over the final and averaging over the initial spin states, the partial width is then given by

$$\Gamma(A \to VP) = (|A_S|^2 + |A_D|^2)PS_2. \quad \text{(C7)}$$

For the V-decay into two pseudoscalar mesons, P_1 and P_2, in the P-wave, the decay amplitude will be given by

$$\mathcal{M}^{1M}_{00}(\Omega_1) = N_1 f^1_{00} D^{1*}_{M,0}(\Omega_1), \quad \text{(C8)}$$

where the helicity amplitude is $N_1 f^1_{00} = \sqrt{3}a_P$.

Correspondingly, averaging over the V-spin states, the partial width is then given by

$$\Gamma(V \to P_1P_2) = |A_P|^2 PS_2. \quad \text{(C9)}$$

APPENDIX D: PHASE SPACE CONVENTION

The nonrelativistic partial width is given by

$$\Gamma(A \to BC) = 2\pi|\mathcal{M}^{(NR)}_{A\to BC}|^2 \times PS_2^{(NR)}, \quad \text{(D1)}$$

where two-body non invariant phase space can be written as

$$PS_2^{(NR)} = \int d^3\vec{k}_B d^3\vec{k}_C \delta^3(\vec{k}_B + \vec{k}_C)\delta(E_B + E_C - m_A) = 4\pi \frac{E_B E_C k_C}{m_A}. \quad \text{(D2)}$$

Since QPCM is in principle a nonrelativistic model and we are using the relativistic Lorentz-invariant tensor formalism to describe $B \to K_1\gamma$ decay, one has to make some kind of continuation. In order to do that, one has to

(i) Use relativistic kinematics (i.e. $E_i^2 = \vec{k}_i^{\,2} + m_i^2$).
(ii) Use relativistic Breit-Wigner forms.
(iii) Make the nonrelativistic decay amplitudes to be "relativistic," correcting the phase space:

$$\Gamma(A \to BC) = \frac{1}{8\pi}\frac{k_C}{m_A^2}|\mathcal{M}^{(R)}_{A\to BC}|^2 = 8\pi^2 \frac{E_B E_C k_C}{m_A}|\mathcal{M}^{(NR)}_{A\to BC}|^2,$$

from which one immediately obtains the relation between the amplitudes:

$$\mathcal{M}^{(R)}_{A\to BC} = 8\pi^{3/2}\sqrt{E_B E_C m_A}\,\mathcal{M}^{(NR)}_{A\to BC}. \quad \text{(D3)}$$

Here, E_i and $\vec{k}_i$ are the energies and momentum, respectively, in the A-reference frame.

[1] M. Gronau and D. Pirjol, Phys. Rev. D **66**, 054008 (2002).
[2] M. Gronau, Y. Grossman, D. Pirjol, and A. Ryd, Phys. Rev. Lett. **88**, 051802 (2002).
[3] E. Kou, A. Le Yaouanc, and A. Tayduganov, Phys. Rev. D **83**, 094007 (2011).
[4] M. Davier, L. Duflot, F. Le Diberder, and A. Rougé, Phys. Lett. B **306**, 411 (1993).
[5] H. Yang *et al.* (Belle Collaboration), Phys. Rev. Lett. **94**, 111802 (2005).
[6] L. Roca, J. E. Palomar, and E. Oset, Phys. Rev. D **70**, 094006 (2004).
[7] R. K. Carnegie, R. J. Cashmore, W. M. Dunwoodie, T. A. Lasinski, and D. W. G. S. Leith, Phys. Lett. **68B**, 287 (1977).
[8] C. Daum *et al.* (ACCMOR Collaboration), Nucl. Phys. **B187**, 1 (1981).
[9] S. Rodeback *et al.* (CERN-College de France-Madrid-Stockholm Collaboration), Z. Phys. C **9**, 9 (1981).
[10] D. Aston *et al.*, Nucl. Phys. **292B**, 693 (1987).

[11] D. A. Bauer *et al.* (TPC/Two Gamma Collaboration), Phys. Rev. D **50**, R13 (1994).
[12] R. Barate *et al.* (ALEPH Collaboration), Eur. Phys. J. C **11**, 599 (1999).
[13] G. Abbiendi *et al.* (OPAL Collaboration), Eur. Phys. J. C **13**, 197 (2000).
[14] D. M. Asner *et al.* (CLEO Collaboration), Phys. Rev. D **62**, 072006 (2000).
[15] H. Guler *et al.* (Belle Collaboration), Phys. Rev. D **83**, 032005 (2011).
[16] B. Aubert *et al.* (BABAR Collaboration), Phys. Rev. D **81**, 052009 (2010).
[17] M. Suzuki, Phys. Rev. D **47**, 1252 (1993).
[18] H. J. Lipkin, *Lie Groups for Pedestrians* (North-Holland, Amsterdam, 1966).
[19] G. L. Kane, Phys. Rev. **156**, 1738 (1967).
[20] G. L. Kane and H. S. Mani, Phys. Rev. **171**, 1533 (1968).
[21] H. G. Blundell, S. Godfrey, and B. Phelps, Phys. Rev. D **53**, 3712 (1996).
[22] S. Godfrey and N. Isgur, Phys. Rev. D **32**, 189 (1985).
[23] H. Hatanaka and K.-C. Yang, Phys. Rev. D **77**, 094023 (2008).
[24] A. Le Yaouanc, L. Oliver, O. Pene, and J. C. Raynal, Phys. Rev. D **8**, 2223 (1973).
[25] L. Micu, Nucl. Phys. **B10**, 521 (1969).
[26] R. D. Carlitz and M. Kislinger, Phys. Rev. D **2**, 336 (1970).
[27] M. B. Gavela, A. Le Yaouanc, L. Oliver, O. Pene, J. C. Raynal, and S. Sood, Phys. Rev. D **21**, 182 (1980).
[28] R. Kokoski and N. Isgur, Phys. Rev. D **35**, 907 (1987).
[29] H. G. Blundell and S. Godfrey, Phys. Rev. D **53**, 3700 (1996).
[30] E. W. Colglazier and J. L. Rosner, Nucl. Phys. **B27**, 349 (1971).
[31] A. Barbaro-Galtieri, in *Proceedings of the Erice Summer School* (Lawrence Berkeley National Laboratory, Berkeley, CA, 1971), p. 581.
[32] B. Silvestre-Brac and C. Gignoux, Phys. Rev. D **43**, 3699 (1991).
[33] M. G. Bowler, J. B. Dainton, A. Kaddoura, and I. J. R. Aitchison, Nucl. Phys. **B74**, 493 (1974).
[34] I. J. R. Aitchison, Nucl. Phys. **A189**, 417 (1972).
[35] S. Godfrey and R. Kokoski, Phys. Rev. D **43**, 1679 (1991).
[36] M. Nauenberg and A. Pais, Phys. Rev. **126**, 360 (1962).
[37] W. R. Frazer and A. W. Hendry, Phys. Rev. **134**, B1307 (1964).
[38] J. Charles, A. Hocker, H. Lacker, S. Laplace, F. R. Le Diberder, J. Malcles, J. Ocariz, M. Pivk, and L. Roos (CKMfitter Group Collaboration), Eur. Phys. J. C **41**, 1 (2005).
[39] K. Nakamura *et al.* (Particle Data Group Collaboration), J. Phys. G **37**, 075021 (2010).
[40] W. Dunwoodie (private communication).
[41] S. Descotes-Genon and B. Moussallam, Eur. Phys. J. C **48**, 553 (2006).
[42] M. Lee *et al.* (Belle Collaboration), Phys. Rev. D **81**, 113007 (2010).
[43] S. U. Chung, "*Spin Formalisms*," CERN 1969.